

# What Has Carbamazepine Taught Crystal Engineers?

Amy V. Hall,\* Aurora J. Cruz-Cabeza,\* and Jonathan W. Steed\*



Cite This: <https://doi.org/10.1021/acs.cgd.4c00555>



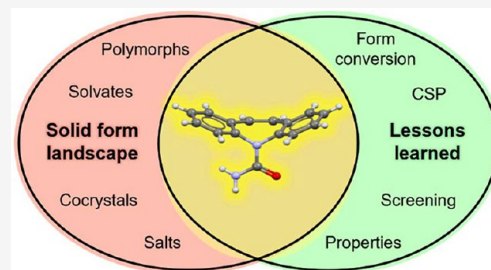
Read Online

ACCESS |

Metrics & More

Article Recommendations

**ABSTRACT:** The antiepilepsy drug carbamazepine is one of the most studied pharmaceuticals in the world. The rich story of its solid forms, cocrystals, and formulation is a microcosm of the topical world of pharmaceutical materials. Understanding carbamazepine has required time, money, and dedication from numerous researchers and pharmaceutical companies worldwide. This wealth of knowledge provides the opportunity to reflect on progress within the crystal engineering field in general. This Perspective covers the extensive solid form landscape of carbamazepine and applies these examples to discuss and answer fundamental questions in the discipline. The story encompasses screening methods, computational solid form discovery, the power and influence of crystal engineering in understanding and controlling crystals and the amorphous state, and the environmental legacy of modern pharmaceuticals. This broad but in-depth analysis of carbamazepine is a vehicle into modern crystal engineering, not only in its own right but across the spectrum of organic materials science and pharmaceutical formulation. Discoveries of carbamazepine demonstrate the potential richness in the materials chemistry of every drug.



## 1. INTRODUCTION

Molecules can be arranged in numerous ways in the solid state, with various relationships existing between different materials. There is the possibility of a broad range of solid forms for a given compound, including polymorphs, amorphous forms, and multicomponent forms, but the questions as to which of these will exist, under which conditions, and how to find and characterize them are areas of ongoing research.<sup>1</sup> Each compound has its own characteristics, and the predictability of a complete solid form landscape based on a consideration of molecular structure alone (before any experimentation) is yet to be realized despite considerable progress in crystal structure prediction calculations.<sup>2,3</sup> A number of fundamental questions in solid-state molecular materials chemistry are only relatively recently being answered, and many still require considerable further research. Why are some compounds highly polymorphic while others are not?<sup>4</sup> Why do some compounds tend to form a broad range of cocrystals while others do not mix with cofomers in the solid state? What can the structure of a form tell us about its crystallization pathway, and what is the role of dynamical and kinetic effects on the form obtained? How can we comprehensively and efficiently screen for solid forms and design new ones? Until a wealth of experimentation and computational work is carried out on each compound, its solid-state behavior remains something of an “unwritten book” despite the fact that each possible material is intrinsically latent in the molecular structure.<sup>5</sup>

In this review, we seek to look at the progress toward answering these fundamental questions using the well-known anticonvulsant drug carbamazepine (CBZ)<sup>6</sup> as a vehicle to drive

the discussion. As a Biopharmaceutical Classification System (BCS) Class II drug with high permeability and low solubility, new and more soluble solid forms of CBZ have been extensively sought after, and what we know and can still learn about CBZ is a microcosm of the state of the art in solid-state molecular materials science in general. The number of crystal structures reported in the Cambridge Structural Database (CSD)<sup>7</sup> that contain CBZ has increased significantly over the last 20 years (Figure 1), and this trend illustrates the diversity and complexity of solid forms often found for drug compounds<sup>8</sup> (Figure 2). The CBZ solid form space includes polymorphs,<sup>9</sup> cocrystals (including ionic cocrystals<sup>10,11</sup> and drug–drug cocrystals<sup>12</sup>),<sup>9,13–26</sup> hydrates,<sup>27</sup> a dihydrate,<sup>28</sup> solvates,<sup>29–32</sup> and salts.<sup>11</sup> CBZ has also been studied in inclusion complexes,<sup>33,34</sup> and in coamorphous systems.<sup>35</sup>

It is not clear what, if anything, makes CBZ a compound uniquely able to crystallize in such a wealth of solid forms. A combination of its awkward shape (resembling a molecular butterfly) together with its hydrogen bonding ability (through its urea group, which in its CBZ bonding environment behaves as a primary amide) appears to both contribute to its extraordinary solid form diversity. However, and perhaps most importantly, it is the fact that a significant amount of time,

**Received:** April 22, 2024

**Revised:** June 3, 2024

**Accepted:** June 12, 2024

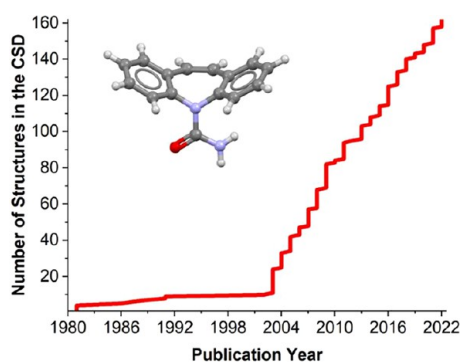


**Figure 1.** Number of crystal structures in the CSD containing CBZ as a function of publication year. The inset shows a molecular model of CBZ.

money, and dedication has been invested in research on the system by numerous research groups around the world.<sup>37</sup> Given the available wealth of knowledge generated by our community on CBZ, here we take the opportunity to reflect on progress in our field with the aid of this iconic system.

## 2. WHAT DO WE KNOW ABOUT CARBAMAZEPINE SOLID FORMS?

**2.1. Overview of CBZ Crystal Forms.** At the time of writing, there are 178 different records of structures containing CBZ in the CSD. After the removal of redeterminations and structures with no coordinates, 114 unique crystal structures of CBZ are classified into the different crystal types shown in Figure 2 with the overall statistics in Figure 3. In terms of crystal compositions and beyond the four single-component (“neat”) polymorphs of CBZ in the CSD, CBZ crystallizes with a wealth of other components: 75% of the cases with one other component, 14% with two, 6% with three and 1% with four other components. The crystal structure with the most components (5 components) is a methanol hydrate of an ionic cocrystal of CBZ with NaI.<sup>10</sup> Structures with 4 components (6 structures) are mostly hydrates of ionic

cocrystals with one of them containing un-ionized CBZ as well as protonated CBZ (CBZ-H<sup>+</sup>).<sup>11</sup> Interestingly, while cocrystals are the largest family of multicomponent systems, only 2-component cocrystals or hydrates and solvates of those have been reported. Thus, a cocrystal of CBZ with three or more nonsolvent components is yet to be prepared. Regarding the stoichiometries of those compositions, the vast majority of the reported forms are stoichiometric with common CBZ:X stoichiometries (given relative to 1 mol of CBZ) being 1:1 and 1:0.5 and common CBZ:X:Y stoichiometries being 1:1:1 and 1:0.5:0.5 (Figure 3). Many structures, however, show disorder with some having unresolved coordinates and stoichiometries for the non-CBZ components.<sup>9</sup> Among those are inclusion compounds of CBZ where CBZ crystallizes in a trigonal framework with the guests disordered in its pores.

CBZ shows a great deal of compositional variation for the given cocrystals. For example, *p*-aminobenzoic acid (pABA) cocrystallizes as a 1:0.5 pure cocrystal with CBZ as well as in a hydrate.<sup>24</sup> Stoichiometric diversity for a fixed set of components is also common in CBZ. For example, with pABA, three distinct stoichiometries can be crystallized (1:1, 2:1, and 4:1).<sup>38</sup> Seven of the 104 crystal compositions containing CBZ exhibit polymorphism (which is ~7%). Among those, pure CBZ is known to exhibit polymorphism as well as its HCl salt and five cocrystals. Regarding salt formation, CBZ is a very weak base as well as a very weak acid. To date, only salts (and ionic cocrystals) where CBZ accepts a proton have been reported. With a pK<sub>a</sub> (protonated base) of ~ -4 and according to the ΔpK<sub>a</sub>, salts where CBZ is protonated would only be expected when paired with very strong acids (with pK<sub>a</sub> < -4).<sup>36</sup> Salts of CBZ have been reported with strong inorganic acids (HCl, HBr) as well as sulfonic acids. The introduction of metals leads to interesting crystalline coordination complexes, where CBZ binds to the metal ions through the amide group.

CBZ exists as four neat polymorphs in the CSD (a fifth form has not been characterized by single-crystal diffraction), one dihydrate, and two other nonstoichiometric hydrates (1:0.3 and 1:0.17). Further statistics on CBZ hydration show that while only 8% of cocrystals are hydrated, ~40% of salts and ionic

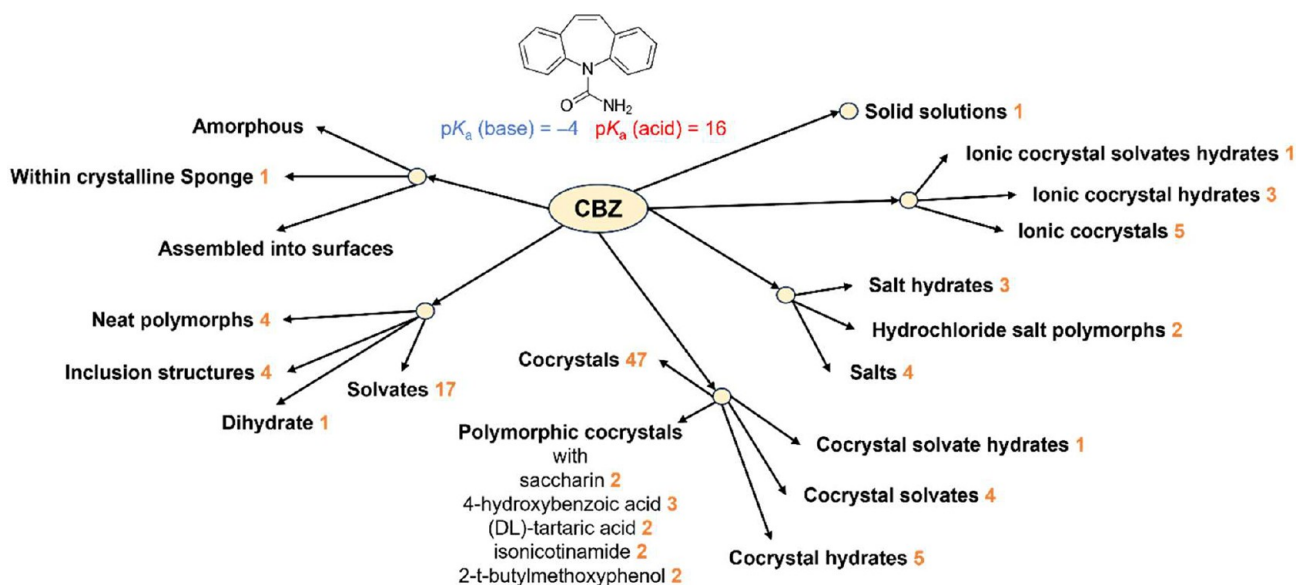


**Figure 2.** An overview of the reported solid forms of CBZ. The number of unique crystal structures in the CSD for each crystal type is given in orange. A total of 114 unique crystal structures. pK<sub>a</sub> values calculated using ChemAxon.<sup>36</sup>

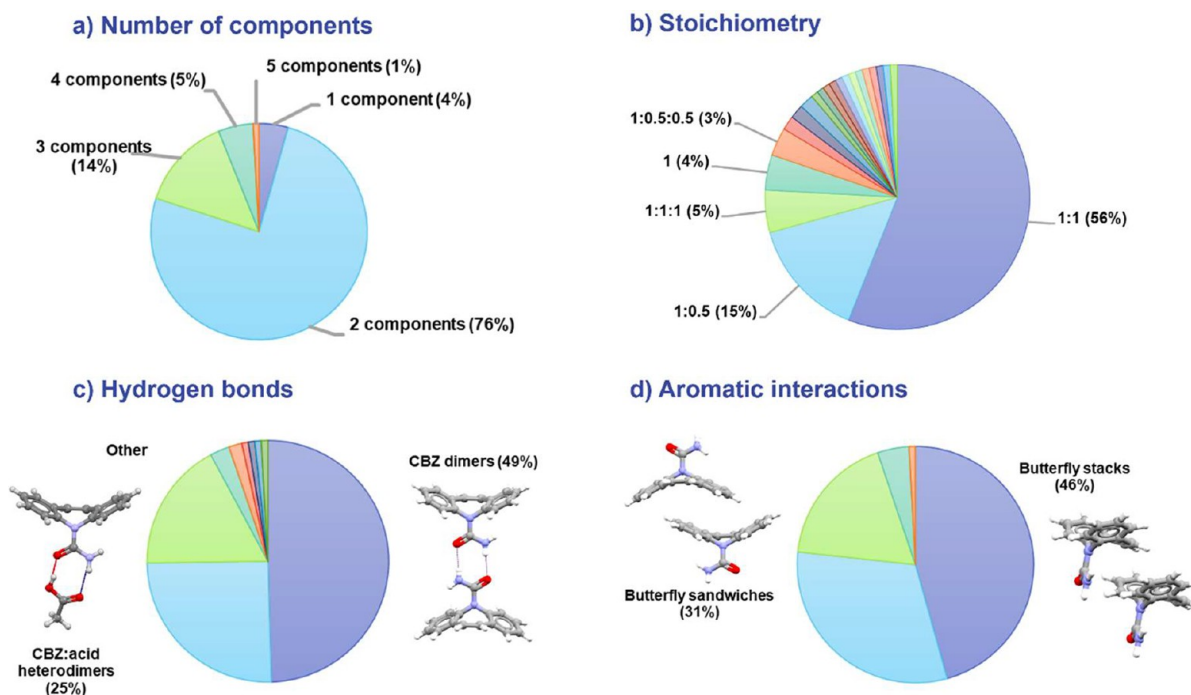


Figure 3. Statistics on CBZ solid forms in the CSD (from 114 unique crystal structures).

Table 1. Summary of Key Information for CBZ Polymorphs

Form	Space group	Z'	CSD Refcode	Computed lattice energy(kJ/mol) <sup>a</sup>	Crystal Morphology	Crystallization
I	$P\bar{1}$ (triclinic)	4	CBMZPN11 <sup>44</sup>	-124.8	Thin Needles	Dominant from the melt
III	$P2_1/c$ (monoclinic)	1	CBMZPN10 <sup>50</sup>	-128.8	Chunks	Dominant from solution at room temperature.
IV	$C2/c$ (monoclinic)	1	CBMZPN12 <sup>51</sup>	-123.3	Plates	Evaporation from methanol solution in the presence of hydroxypropyl cellulose and from the melt. Robustly produced from amorphous CBZ.
V	$Pbca$ (Orthorhombic)	1	CBMZPN16 <sup>48</sup>	-124.7	Plates	Templated on the crystal of an analogue from vapor growth (Elusive)
VI	—	—	—	—	Coarse spherulites	From the melt (Elusive)

<sup>a</sup>Computed with the FIT potential using atomic multipoles.<sup>48</sup>

cocrystals contain water. These statistics reconfirm within the microcosm of CBZ solid forms the importance of charge for the uptake of water in molecular crystals.<sup>39</sup>

An analysis of dominant recurrent interactions within all 114 unique crystal structures containing CBZ in the CSD reveals that the dominant motifs containing CBZ are (i) CBZ hydrogen bonded (HB) dimers, (ii) CBZ aromatic stacks, and (iii) CBZ sandwiches (Figure 3c and d). In the HB dimers, two molecules of CBZ interact through two hydrogen bonds formed with the carboxamide group (Figure 3c) to form an  $R_2^2(8)$  motif, the molecules most usually being related by inversion symmetry. These dimers leave an acceptor site and a donor site available to further interact with other components. Thus, in multi-component systems, typically two scenarios are possible: a) either the homodimer is broken in favor of a heterodimer (typically when the second component contains a carboxylic acid) or b) the homodimer is retained, and the second component interacts with the available side donor and acceptor (most common in CBZ solvates and hydrates). The aromatic structure in CBZ is very dominant, and thus aromatic interactions are key in CBZ crystal forms. Here, the CBZ molecules can either stack, making use of translation symmetry,

or form aromatic sandwiches (with  $\text{CH}\cdots\text{ring}$  as well as parallel displaced aromatic stacking interactions), making use of inversion symmetry. While the stacks propagate infinitely in the lattice, thus constituting a strong interaction that will contribute to the kinetics of crystal growth, the sandwiches are dimers and do not propagate. Despite the presence of other components in the crystal structures, in nearly 80% of crystals containing CBZ, either the aromatic stacking or the aromatic sandwich interaction remains.

**2.2. Amorphous CBZ.** CBZ can exist in the amorphous state (CBZ-A) either on its own or with other components (coamorphous). Pure CBZ forms a relatively strong glass which can be generated either by quench cooling or from dehydration of CBZ dihydrate (at low relative humidity and below the glass transition temperature of around 56 °C).<sup>40</sup>

Coamorphous phases containing CBZ have also been widely reported. Among them, there are studies with saccharin,<sup>41</sup> lactose,<sup>41</sup> gluconolactone,<sup>41</sup> nicotinamide,<sup>42</sup> benzoic acid, maleic acid, succinic acid, tartaric acid, and saccharin to name a few.<sup>43</sup> While some of these materials are stable phases, others easily convert back to cocrystals. Additionally, a coamorphous phase of an ionic cocrystal with citric acid and L-arginine has



been reported.<sup>35</sup> This ionic coamorphous phase has a dramatically increased glass transition temperature relative to that of pure CBZ or other coamorphous materials.

**2.3. Neat Polymorphs of CBZ.** At present, five crystalline anhydrous forms of pure CBZ have been reported (I, III, IV, V, and VI) with four of them having single crystal structures in the CSD (Table 1). CBZ polymorphism and nomenclature of the first three polymorphs (I, III, and IV) were reviewed in 2003 in the seminal paper by Greziak et al.<sup>44</sup> together with the so-called form II. In subsequent work, however, what was once believed to be the anhydrous form II of CBZ (the trigonal form with CSD refcode CBMZPN03)<sup>45</sup> was shown to be an inclusion solvate with highly disordered solvent molecules within its hydrophobic channels.<sup>46,47</sup> As such, form II is not technically a polymorph of anhydrous CBZ and will not be discussed further in this section. Forms V and VI were discovered after the 2003 review.<sup>48,49</sup>

From the historical analysis presented by Greziak et al. in 2003,<sup>44</sup> forms I and III CBZ appear to have been reported in many independent works from as early as 1968.<sup>52</sup> They are related enantiotropically with a transition temperature of  $\sim 71$  °C, with form III being the low-temperature form.<sup>53</sup> Form III can be typically produced by crystallization from solution under a wide range of experimental conditions, giving rise to chunky blocks whose structure was first determined in 1981.<sup>54</sup> Because of its dominance under ambient conditions, form III is the most commonly found commercially. Form I dominates at high temperatures, especially in crystallization from the melt. Although form I was reported very early (1968), it grows as very thin needles whose structure was not determined until 2003.<sup>44</sup>

The remaining forms (IV, V, and VI) are metastable and more elusive in nature. Although there exists rare evidence of form IV as early as 1987,<sup>55</sup> this polymorph was not fully isolated and characterized until 2002. Good quality single crystals of form IV were obtained by evaporation from methanol solutions in the presence of hydroxypropyl cellulose.<sup>51</sup> Form IV can also be consistently obtained by crystallization from amorphous CBZ<sup>56</sup> and by finger-touched assisted ball-mill grinding.<sup>57</sup> Form V was first (and solely) reported in 2011.<sup>48</sup> The discovery of form V deserves careful analysis, and it will be discussed in detail later; it remains one of the few examples in the literature of polymorph discovery predicted and enabled by computation. It has only been produced once by vapor growth using templation on a closely related analogue.<sup>48</sup>

Finally, form VI has only been reported recently (2022); it was produced by crystallization from the melt, and its structure remains undetermined.<sup>49</sup> Fella et al. showed that forms I, III, IV, and VI can all be obtained from the melt (often concomitantly), and Broadhurst et al. showed with TEM that forms I, III, and IV can be crystallized concomitantly.<sup>58</sup>

**2.4. CBZ Dihydrate.** The dihydrate of CBZ is the most stable form at relative humidity above 40% and below the CBZ glass transition temperature ( $\sim 56$  °C).<sup>56</sup> Because of its greater stability, CBZ dihydrate (CBZ-DH) is around 1.4–1.6 times less soluble than the most common anhydrous forms CBZ-III and -I.<sup>59</sup> CBZ-DH also has a lower dissolution rate. Because of this, the unwanted presence of CBZ-DH in tablet formulations is a cause of major concern for CBZ delivery since it can significantly affect the drug's bioavailability. Exposed to high relative humidities (RH > 80%), tablets containing CBZ-III are known to start converting to the CBZ-DH after 2 days, with full conversion occurring after only 5 days.<sup>60</sup>

A long-standing topic of debate about CBZ-DH concerns its crystal structure. The structure of a CBZ dihydrate was first reported in 1986 (FEFNOT, R = 10%)<sup>61</sup> in the orthorhombic space group *Abam* (nonstandard setting of *Cmca*). Nearly 20 years later (2004), CBZ-DH was redetermined in the *Cmca* space group (FEFNOT01, R = 4.3%) and described as an order–disorder structure in which, for the hydrogen bonding to be optimized, two types of layers should exist (whereby the amide group is rotated by  $180^\circ$ ) distributed randomly in the structure.<sup>61</sup> A year later (2005), a combined X-ray diffraction and solid-state NMR study described the structure as ordered in the  $P2_1/c$  space group (FEFNOT02, R = 7.3%) arguing that the disordered effects seen could be a consequence of twinning.<sup>28</sup> A more recent (2015) detailed neutron and high-resolution X-ray diffraction study now favors the disordered *Cmca* structure over the ordered (but twinned)  $P2_1/c$  structure.<sup>62</sup> The authors, however, highlight that there is the possibility that “the degree of disorder and twinning varies from crystal-to-crystal specimen” in CBZ-DH. The CBZ-DH structure is a testimony of the experimental and theoretical difficulties encountered when even simple systems show disorder and/or twinning, which is a relatively common (yet often unaddressed) phenomenon. CBZ-DH has been reported to grow with marked anisotropy with reported morphologies ranging from laths to thin needles depending on the growth conditions.<sup>19</sup> Early reports have suggested that CBZ-DH needles grow with a whisker mechanism.<sup>63</sup>

**2.5. Inclusion Structures (Trigonal CBZ).** The trigonal ( $R\bar{3}$ ) form of CBZ (CBZ-t) was originally reported as a pure polymorph of CBZ (form II, CBMZPN03)<sup>45</sup> but later realized (by two independent studies)<sup>46,47</sup> to contain heavily disordered guest compounds (typically solvents) in its structural channels. CBZ-t is, therefore, an inclusion framework whose structure varies slightly depending on the solvent trapped in the hydrophobic channels (Figure 4, with the diameter of the

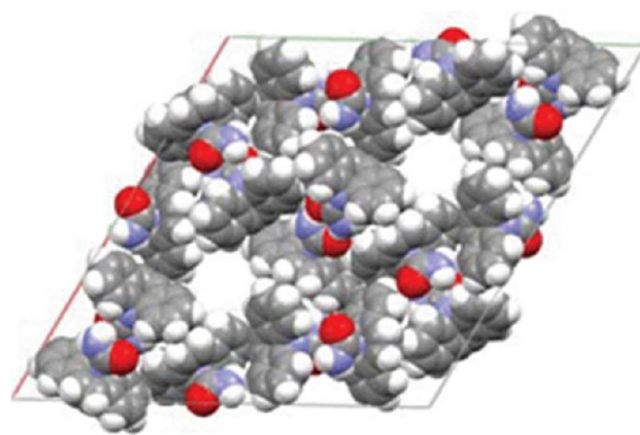


**Figure 4.** A space fill representation of trigonal CBZ displaying its structural pores along the *c*-axis. Figure reproduced from reference 46 with permission from the Royal Society of Chemistry.

channels adjusting from 5.7 to 7.7 Å).<sup>27</sup> The presence of solvent in the CBZ-t channels has been shown to be key for the formation and stability of these inclusion structures of CBZ-t.<sup>46</sup> The CBZ-t structure has been reported for guests such as toluene, tridecane, and tetrahydrofuran (MIMQIJ).<sup>47</sup> Surprisingly, CBZ-t has also been reported to form with water nanowires acting as guests in 1:0.33 and 1:0.17 stoichiometries (PEYSOD,<sup>27</sup> YADZAH<sup>64</sup>). Given how hydrophobic the CBZ-t

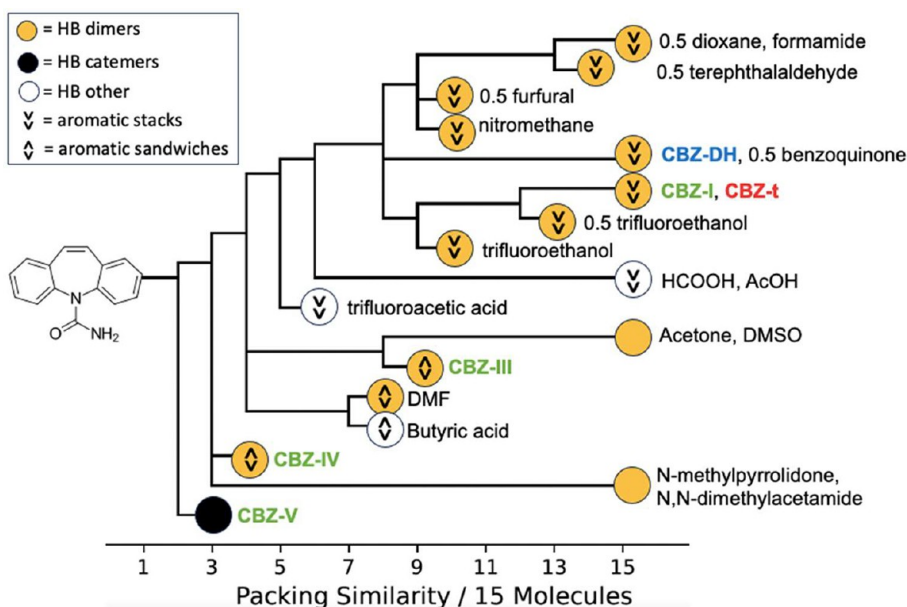


**Figure 5.** Crystal packing similarity dendrogram<sup>9</sup> for CBZ polymorphs (green), trigonal CBZ inclusion framework (red), and CBZ solvates (black). Twenty-three crystal structures are listed in total. Yellow circles are CBZ HB dimers, black circles are CBZ HB catemers, and white circles are CBZ hydrogen bonded to another component (typically forming heterodimers with acids). Symbols within the circles indicate the aromatic interactions (CBZ aromatic stacks  $\llcorner$ , or CBZ aromatic sandwiches  $\triangleleft$ ). If not indicated, CBZ:solvent stoichiometries are 1:1 except when a 0.5 is given, which is then 1:0.5.

pores are, it is surprising that water is included in the channels stabilizing the structure and reminiscent of water nanowires in carbon nanotubes.<sup>65</sup>

**2.6. Solvates of CBZ.** CBZ is also a prolific solvate former. Due to CBZ's nature as a primary amide, the CBZ HB dimers leave a pair of HB donor and acceptor sites at the periphery which are unsatisfied in its neat forms. This occurs because of geometric constraints within the molecule. Consequently, in many of its solvates, CBZ exists as HB dimers with further side hydrogen bonds to the solvents via the remaining amide NH proton and to fill the space between adjacent amide dimer pairs.

Beyond water, other solvents that cocrystallize with CBZ into solvate structures include polar solvents able to accept hydrogen bonds (acetone,<sup>29</sup> benzoquinone,<sup>29</sup> DMF,<sup>66</sup> DMSO,<sup>29</sup> formamide,<sup>29</sup> *N*-methylpyrrolidone,<sup>67</sup> *N,N*-dimethylacetamide,<sup>67</sup> furfural,<sup>68</sup> dioxane,<sup>19</sup> nitromethane,<sup>67</sup> and terephthalaldehyde<sup>29</sup>), trifluoroethanol in two stoichiometries (1:1 and 1:0.5, SAPDUJ<sup>69</sup> and ELIVON<sup>30</sup>), and liquid carboxylic acids (formic acid,<sup>29</sup> acetic acid,<sup>29</sup> trifluoroacetic acid,<sup>70</sup> and butyric acid<sup>29</sup>).

CBZ is not unique in its ability to form multiple solvates, as other prolific solvate-forming compounds exist. For example, the sulfa drug sulfathiazole has over 100 solvate structures,<sup>71</sup> alongside 101 crystal structures which include sulfathiazole polymorphs, cocrystals, and salts.<sup>72</sup> Additionally, the antipsychotic drug olanzapine has been crystallized in at least 60 different forms, with 35 crystal structures of the solvated forms,<sup>73,74</sup> while the cancer drug Galunisertib has been crystallized as more than 50 different solvates and 10 polymorphs.<sup>75</sup>

**2.7. Structural Similarities between CBZ Neat Forms, Inclusion Forms, and Solvates.** CBZ neat forms, trigonal forms, and CBZ solvates were compared using the COMPACK algorithm with standard settings and clusters of 15 molecules.<sup>76</sup> The results of these comparisons are illustrated in the form of a packing similarity dendrogram (Figure 5) in which node symbols indicate the type of interactions between CBZ

molecules present in the different structures. This analysis is a simplified version of the comparisons done by Childs et al.<sup>9</sup> or Gelbrich and Hursthouse;<sup>77</sup> here, we only report on polymorphs and solvates (no cocrystals).

The comparisons illustrate that there is a high degree of similarity between many of these CBZ structures and, in many cases, full isostructurality. In the case of solvates, for example, the dioxane and formamide solvates, the CBZ-DH and benzoquinone solvate, the acetic acid and formamide solvates, and the *N*-methylpyrrolidone and *N,N*-dimethylacetamide solvates are all isostructural. In the case of neat polymorphs, CBZ-I has a high degree of similarity with CBZ-t. Overall, the CBZ HB dimers assembled with aromatic stacks are the dominant recognition modes in many of these structures. The least common interactions are observed in two of the neat polymorphs: CBZ-IV and CBZ-V, which are known to be harder to crystallize. Especially CBZ-V is rare since it is the only structure where CBZ hydrogen bonds using a catemeric motif rather than a dimer.

**2.8. Cocrystals of CBZ.** Cocrystallization offers the opportunity to adapt and improve the physicochemical properties (e.g., solubility,<sup>78,79</sup> dissolution,<sup>80–83</sup> and stability<sup>84</sup>) of compounds without the need for covalent modification,<sup>85</sup> an especially attractive strategy for drug delivery.<sup>86</sup> Considering all of the different subsets of multicomponent solids containing CBZ, CBZ cocrystals are the most abundant in the CSD (69 structures of cocrystals and their solvates and hydrates). CBZ cocrystals have been reported with a wide range of coformers including *p*-benzoquinone,<sup>19,29</sup> formamide,<sup>29</sup> methylparaben,<sup>87</sup> hydroxyanisole,<sup>87</sup> mono- to tetra-carboxylic acids,<sup>9,29,87–89</sup> and a wide variety of flavonoid molecules.<sup>90,91</sup> The very many cocrystal structures of carbamazepine are instructive because Etter's rules<sup>92</sup> are not obeyed in around a quarter of cases as a result of the steric hindrance caused by the CBZ butterfly ring (dibenzazepine group).<sup>9</sup>

Of all 69 unique cocrystals with a known crystal structure, 62% (43) are with coformers containing a carboxylic acid. While

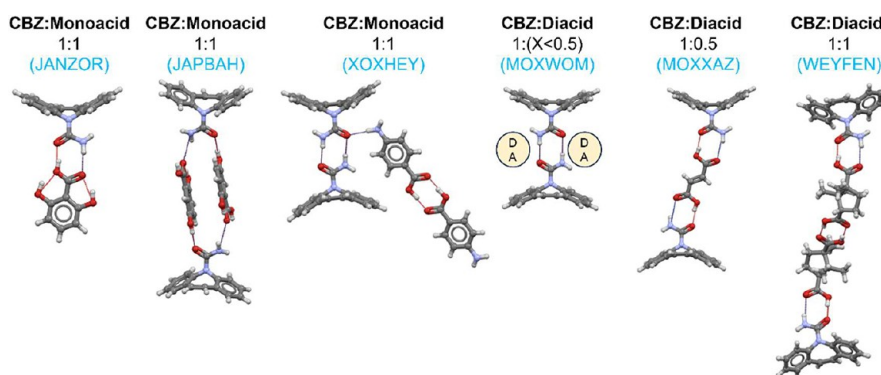


Figure 6. Diversity of HB assemblies for CBZ cocrystals with carboxylic acids.

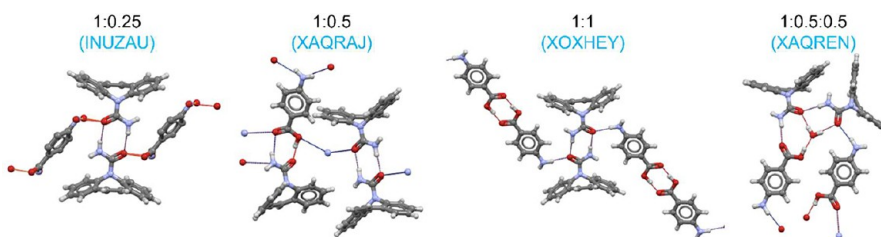


Figure 7. Diversity of hydrogen bonding found in cocrystals of CBZ:pABA.

53% of those structures (23) form CBZ-acid heterodimer motifs,<sup>24</sup> the composition and stoichiometry of the system play a role in the overall outcome (Figure 6). Thus, monocarboxylic acids with no other accepting–donating capabilities present in a CBZ:Acid 1:1 ratio will most likely form the heterodimer (Figure 6, JANZOR).<sup>88</sup> Since cocrystal structures in the CSD are dominated by systems for which we can rationalize interactions, it is not surprising that this group of cocrystals containing simple acids and heterodimer motifs with CBZ dominates. More interesting, perhaps, are those systems that break our preconceived crystal-engineering rules. Thus, when the compounds contain other donor–acceptor groups (Figure 6, JAPBAH<sup>88</sup> and XOXHEY<sup>25</sup>), unpredictable motifs to the biased crystal engineering mind start to appear. The composition also plays a role. For example, diacids present in small fractions relative to CBZ are known to leave the CBZ-dimer untouched and simply form side hydrogen bonds with CBZ in a structure similar to that of CBZ-DH.<sup>9</sup> 1:0.5 (MOXWOM and MOXXAZ)<sup>9</sup> and 1:1 (WEYFEN)<sup>93</sup> stoichiometries can also be accommodated in diacids with the heterodimer motif (Figure 6).

Another example of unexpected outcomes and interaction diversity can be seen in the cocrystals of CBZ with pABA as neat 1:0.25 (INUZAU),<sup>38</sup> 1:0.5 (XAQRAJ),<sup>24</sup> and 1:1 (XOXHEY)<sup>25</sup> cocrystals can be made. The 1:0.25 cocrystal consists of CBZ homodimers, with pABA interacting with them through side HBs. The 1:0.5 cocrystal contains both the CBZ homodimers and the CBZ:pABA heterodimer, while the 1:1 cocrystal contains CBZ homodimers and pABA homodimers. A monohydrate of the 1:1 (XAQREN)<sup>24</sup> cocrystal also exists with its hydrogen bonding interactions being largely unpredictable (Figure 7).

Most importantly, 81% of compounds crystallizing with CBZ contain an aromatic ring. Aromatic interactions are very important in CBZ, with 77% of all CBZ-containing crystal structures showing either CBZ–CBZ butterfly ring stacks or CBZ–CBZ butterfly sandwiches (Figure 3d). In the absence of

or in conjunction with these dominant CBZ–CBZ aromatic interactions, aromatic cofomers can interact with the butterfly ring either by sitting on top or under the azepine ring.<sup>9</sup> It is, perhaps, unsurprising that cofomers able to both hydrogen bond and aromatic stack are thus able to effectively form cocrystals with CBZ.

Cocrystals can also exhibit polymorphism. Examples of polymorphic CBZ cocrystals in the CSD are CBZ with tartaric acid (MOXWIG/01),<sup>9,94</sup> isonicotinamide (LOFKIB/01),<sup>95,96</sup> 2-*t*-butyl-4-methoxyphenol (HEDYIC/01),<sup>87</sup> and saccharin (UNEZAO/01).<sup>29,97</sup> The 1:1 CBZ:saccharin cocrystal polymorphs are interesting examples. Form I retains the CBZ–CBZ homo-H-bonded dimers but contains heteroaromatic CBZ–saccharin interactions, whereas form II has CBZ–saccharin hetero-H-bonded dimers with homoaromatic CBZ–CBZ and saccharin–saccharin interactions (Figure 8). The 1:1 CBZ:saccharin forms I and II are related monotropically with form I being the most stable and form II easily converting to form I.<sup>98</sup>

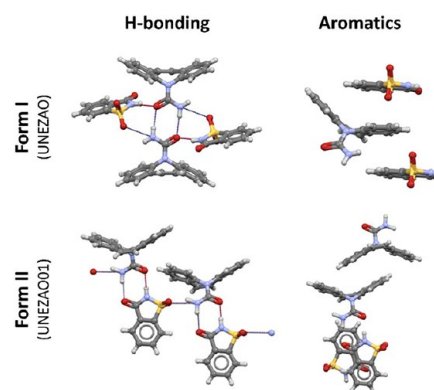


Figure 8. H-bonding and aromatic interactions found in 1:1 CBZ:saccharin form I (UNEZAO)<sup>29</sup> and 1:1 CBZ:saccharin form II (UNEZAO01).<sup>97</sup>



Form I (plates) can be readily crystallized by slow evaporation from solution of equimolar amounts of CBZ and saccharin, while form II was first obtained by crystallization from solution in the presence of polymers. Spray drying techniques can selectively produce either of the CBZ:saccharin cocrystal forms, electro-spraying produces a mixture of forms, while supercritical CO<sub>2</sub>-assisted spray drying produces form I only.<sup>99</sup> Interestingly, the 1:1 CBZ:thiosaccharin cocrystal is isostructural with 1:1 CBZ:saccharin form I but not form II, illustrating that the replacement of the carbonyl oxygen atom with a sulfur atom results in isostructural or isomorphous forms.<sup>26</sup>

**2.9. CBZ–Drug Cocrystals.** Drug–drug cocrystals have incredible potential to enhance the physicochemical properties of existing drugs and combine two different therapeutic treatments into a single simple crystalline dose. While still scarce in the literature, they are becoming more common.<sup>100</sup> Ten different examples of drug–drug cocrystals containing CBZ are given in Table 2. An interesting example is the CBZ–chlorothiazide

**Table 2. CBZ:Codrug Cocrystals Currently Reported in the Literature and the CSD**

Drug Coformer	Drug Coformer Class	CSD Refcode
Aspirin	NSAID	TAZRAO <sup>15</sup> and TAZRAO01 <sup>102</sup>
Indomethacin	NSAID	LEZKEI <sup>103</sup>
Ketoprofen	NSAID	RAFGIS <sup>14</sup>
Celecoxib	NSAID	n/a—no X-ray structure <sup>104</sup>
Chlorothiazide	Diuretic	VEJZUI <sup>101</sup>
<i>p</i> -aminosalicylic acid	Antibiotic	FAYXOV <sup>13</sup>
Pyrimethamine	Antimalarial	KICWOK <sup>105</sup>
Emodin	Anti-inflammatory (traditional medicine)	MEXMOV <sup>106</sup>
Paeonol	Anti-inflammatory (traditional medicine)	MEXMUV <sup>106</sup>
Apigenin	Anticancer (traditional medicine)	JINHIB <sup>107</sup>

cocrystal, synthesized by mechanochemical methods and with crystals grown by slow evaporation from acetone.<sup>101</sup> The structure is actually a 2:1:0.5:0.5 CBZ:chlorothiazide:acetone:water cocrystal solvate hemihydrate (VEJZUI) with a very complex asymmetric unit containing four CBZ, two chlorothiazide, one acetone, and one disordered water molecules. In this structure, the CBZ:CBZ H-bonded dimers and aromatic stacks are maintained, and the structure resembles that of a modified inclusion CBZ structure, where the codrug together with the two solvent molecules sit in the structural pores. This 2:1:0.5:0.5 CBZ:chlorothiazide:acetone:water cocrystal solvate hemihydrate has an enhanced dissolution profile compared to the two separate isolated drugs.<sup>101</sup>

Artificial intelligence and machine learning (AI ML) prediction tools are increasingly used to screen drug–drug interactions in an effort to optimize the drug discovery process. An example of using AI ML computations to predict drug–drug cocrystals is the CBZ–ketoprofen cocrystal.<sup>14</sup> Until this point, ketoprofen had not been cocrystallized. Following the *in silico* prediction methods, the cocrystal was successfully synthesized by mechanochemical grinding (RAFGIS).<sup>14</sup>

**2.10. Salts and Ionic Cocrystals of CBZ.** In addition to neutral cocrystals, CBZ also forms a range of salts and ionic cocrystals with NH<sub>4</sub><sup>+</sup>, oxonium, and sodium cations. The ionic CBZ cocrystal with NaI involves a complex in which the Na<sup>+</sup>

is coordinated to four CBZ molecules via polar amide oxygen atoms as a mixed methanol–water solvate. Ionic CBZ cocrystals are also known with pentacoordinated sodium as the I<sub>3</sub><sup>−</sup> salt and a double salt with acridinium and IBr<sub>2</sub><sup>−</sup> (DOXDAX, Figure 9a).<sup>10</sup> The high ratio of CBZ to the salt conformer is

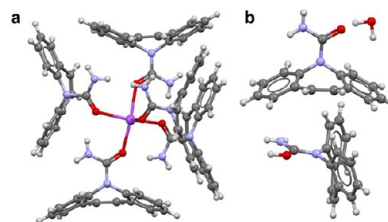


**Figure 9.** (a) Pentacoordinate Na<sup>+</sup> ion in [Na(CBZ)<sub>5</sub>][I<sub>3</sub>] and (b) CBZ ionic cocrystal in CBZ·[CBZ(H)][BF<sub>4</sub>]<sup>−</sup>·0.5H<sub>2</sub>O.<sup>10,11</sup>

interesting from the point of view of drug form selection. While solubility measurements have not been reported, salts are likely to be more water-soluble than neutral CBZ. CBZ also forms 1:1 ionic cocrystal with NH<sub>4</sub>X (X = Cl, I), and an oxonium ion salt [H<sub>3</sub>O][Cl]·2CBZ·2H<sub>2</sub>O. All of these materials involve the well-known CBZ:CBZ H-bonded homodimer which also accommodates hydrogen bonding from the small ammonium ion. In contrast, in the polyiodide [acridinium][I<sub>3</sub>]<sup>−</sup>·CBZ·2.5I<sub>2</sub>, the bulky acridinium NH<sup>+</sup> group hydrogen bonds with the CBZ carbonyl oxygen atom, and hence the dimer motif is lost.<sup>11</sup>

The basicity of the CBZ amide oxygen atom also means that it can be protonated rather than complexed with H<sub>3</sub>O<sup>+</sup> in the presence of strong acids. In these complexes, the CBZ dimer motif is lost because of the protonation. Reaction with HCl and HBr gives rise to hydrochloride and hydrobromide salts (both of which exist as two polymorphs), and species such as a hydrate [CBZ(H)][Cl]·H<sub>2</sub>O. In the halide salts, the eight-membered hydrogen-bonded CBZ dimer ring is replaced by an R<sub>2</sub><sup>1</sup>(6) motif in which the amide NH and protonated OH both hydrogen bond to the anions.<sup>108</sup> Cocrystallization with HBF<sub>4</sub> results in a different kind of ionic cocrystal CBZ·[CBZ(H)][BF<sub>4</sub>]<sup>−</sup>·0.5H<sub>2</sub>O in which a neutral CBZ molecule is cocrystallized with protonated CBZ as the BF<sub>4</sub><sup>−</sup> salt (HUQWOH, Figure 9b). A series of sulfonic acid salts are also known [CBZ(H)]·[O<sub>3</sub>SC<sub>6</sub>H<sub>5</sub>], [CBZ(H)][O<sub>3</sub>SC<sub>6</sub>H<sub>4</sub>(OH)]·0.5H<sub>2</sub>O, [CBZ(H)]<sub>2</sub>[O<sub>3</sub>SCH<sub>2</sub>CH<sub>2</sub>SO<sub>3</sub>], and [CBZ(H)][O<sub>3</sub>SC<sub>6</sub>H<sub>3</sub>(OH)(COOH)]·H<sub>2</sub>O which generally form eight-membered hydrogen-bonded rings between the protonated amide and −SO<sub>3</sub><sup>−</sup> group.<sup>11</sup> Salt and cocrystal formation have been studied in the context of attempts to modify the solubility and biological activity of CBZ. As part of this work, the 1:1 picrate (trinitrophenolate) salt was prepared and found to involve a strong hydrogen bond from the protonated amide to both the phenolate oxygen atom and one of the nitro groups. Biological studies were not pursued, however, because of the toxicity of picrate.<sup>109</sup>

### 3. WHAT HAS CARBAMAZEPINE TAUGHT US?

The tremendous diversity in CBZ solid-state chemistry and the varied and creative ways in which CBZ forms have been discovered over the past half-century teach us some general lessons that permeate the entire field of molecular solid-state chemistry. The emergence of such a varied array of solid forms of this drug highlights the necessity of exploring and developing very diverse and (with the aid of CSP) targeted crystallization

methods for solid form screening and control.<sup>110,111</sup> For example, high throughput methods,<sup>112</sup> high pressure,<sup>113,114</sup> nanoconfinement,<sup>115,116</sup> encapsulated nanodroplet crystallization,<sup>117</sup> microgel crystallization,<sup>118</sup> milling approaches,<sup>119</sup> polymer templating,<sup>120,121</sup> heteroseeding from the melt,<sup>122</sup> mixed molecular crystallization,<sup>123,124</sup> as well as crystallization in supramolecular gels,<sup>125</sup> microemulsions,<sup>126</sup> structured-ternary fluids,<sup>127</sup> deep eutectic solvents,<sup>128</sup> and in the presence of magnetic fields.<sup>129</sup> In addition, the example of CBZ Form V shows that molecular analogues of target compounds can be very powerful in bringing about thermodynamic control, templation, and solid form discovery. Work on CBZ also highlights how important it is to understand crystallization pathways, while the diversity of multicomponent crystalline and amorphous forms of CBZ illustrate the power of crystal engineering to influence solid-state properties. Finally, CBZ is not always beneficial; like many widespread drugs, it is becoming a source of environmental concern.<sup>130</sup> We address each of these topics in detail below.

**3.1. The Necessity of Diverse Crystallization Methods for Screening and Control.** High throughput, automated crystallization methods are increasingly powerful and routinely applied in solid form screening. As early as 2006, an automated parallel crystallization search was applied to carbamazepine. This study covered 66 solvents and five crystallization protocols, analyzing the results using principal component analysis (PCA). This resulted in the identification of CBZ-I, CBZ-t, and CBZ-III as well as the CBZ-DH and eight organic solvates, including three new solvate forms (N,N-dimethylformamide (1:1); hemifurfural; hemi-1,4-dioxane).<sup>112</sup> For CBZ, the solvent type played relatively little role in the polymorphs obtained, except in cases where it was directly incorporated. This systematic study also showed that previous reports of polymer templating of CBZ-IV were not reproducible, highlighting the stochastic nature of the nucleation process and potential pitfalls of drawing conclusions from limited data. It is worth noting that this study was supported by computational CSP which showed that the catameric hydrogen-bonded CBZ chain motif was common and stable. Since no catameric structures were known at the time, the authors concluded that kinetics favor nucleation of crystal structures based on the CBZ–CBZ  $R_2^2(8)$  hydrogen-bonded dimer motif. It was not until 2011 that heteroseeding allowed the targeted experimental realization of CBZ-V.

The control of different CBZ forms has also been possible by crystallization in supramolecular gels.<sup>125</sup> Four different bis-(urea) gelators were combined in various solvents with CBZ and heated, with gels forming on cooling. Large, well-defined crystals of CBZ formed in the transparent gels and crystallized in either the CBZ-t form or the thermodynamic CBZ-III, depending on the concentration of CBZ in the sample (higher concentrations of CBZ formed polymorph CBZ-t, while lower concentrations formed CBZ-III). In one particular gel, the crystallization of the high-temperature CBZ-I was observed under conditions that typically give rise to CBZ-DH in solution. Formation of CBZ-I (typically obtained from the melt) under ambient conditions is uncommon. The large single crystals produced in the gels were recovered by anion-switching. The presence of tetrabutylammonium acetate as a solid on top of the gel led to the rapid dissolution of the gel which then allowed for the recovery of the crystals for analysis by X-ray diffraction (Figure 10).<sup>125</sup>

Interestingly, the formation of metastable CBZ-I can also be brought about by crystallization in the presence of a magnetic field (>0.6 T). A similar effect occurs for flufenamic acid at

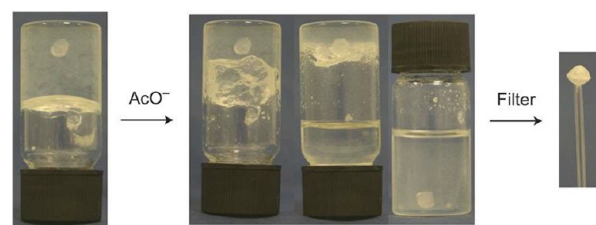


**Figure 10.** A large CBZ crystal (form III) grown in a supramolecular gel. The gel is dissolved by acetate ions to retrieve the large single crystal for X-ray diffraction. Figure reproduced with permission from reference 125.

around 1 T, but the magnetic field does not affect the crystallization of the closely related mefenamic acid. The role of the magnetic field lies in the different diamagnetic susceptibilities of crystallites of different polymorphs of a given compound. For CBZ, at higher magnetic field strength, the onset of crystallization (determined by turbidity measurements) occurs at lower temperatures and hence greater supersaturation. As a result, the magnetic field causes crystallization of the metastable form in a way analogous to Ostwald's rule of stages.<sup>131</sup>

CBZ has also been studied by the relatively neglected technique of melt crystallization, including melting under nanoconfinement. CBZ was one of 21 extensively polymorphic, well-documented substances possessing at least five known forms studied by melt crystallization. This work revealed over half of the recognized polymorphs and even unveiled fresh polymorphs that had eluded detection through alternative screening methods (Figure 11). Melt-grown polymorphs tend to have higher  $Z'$  values, which can be a particular problem for CSP methods. For CBZ in particular, Forms I, III, IV, and a new form dubbed Form VI occurring as coarse spherulites could be isolated from the melt, with Form I (the stable form at high temperatures) dominating. When melt crystallization was conducted within nanopores ranging from 8 to 100 nm, 19 of the 21 compounds predominantly yielded polymorphs that mirrored those formed in the bulk melt at similar temperatures, but melt crystallization under confinement also produced new polymorphs that had eluded discovery by other crystallization approaches. This proved true for CBZ which gave the metastable CBZ-I in larger pores and a new form (yet to be characterized) in 8 nm pores.<sup>49</sup> The role of particle size which can be explored by different means including nanoconfinement<sup>132</sup> and milling<sup>133</sup> is thus also important for the production of novel polymorphs in CBZ.

One particularly exciting recent development in crystallization methods under confinement is the use of encapsulated nanodroplet crystallization, which involves nanoliters of solution injected into an inert oil medium to control the rate of solvent loss (ENaCt, Figure 12).<sup>134</sup> The method has yet to be applied to CBZ but used as a test case for an even more well-known and highly polymorphic compound beloved by crystal engineers, the olanzapine precursor ROY (so-called because of the red, orange, and yellow colors of its many solid forms). The almost simultaneous publication of new ROY polymorphs produced by ENaCt and mixed crystal heteroseeding<sup>122</sup> in 2020 brought the total number of known ROY nonsolvated polymorphs to 14, 12 of which have been characterized by single-crystal X-ray diffraction over the past 25 years.<sup>135</sup> The ENaCt grown ROY polymorph R18 has a surprising near-planar conformation, suggesting it to be highly metastable. Designer supramolecular





**Figure 11.** Polarized optical micrographs of melt-grown solid forms. CBZ is shown in E. Reproduced from reference 49. Copyright 2022 American Chemical Society.

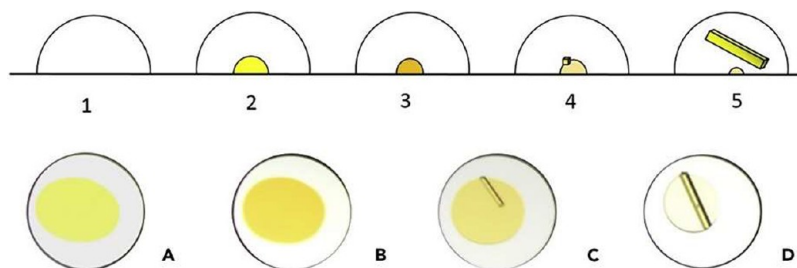


**Figure 12.** A cross-section schematic of the oil-encapsulated nanodroplet crystallization experiment. Figure reproduced with permission from reference 134.

gels and microgel particles can also control the polymorphic form of ROY.<sup>118,136</sup>

Nanoconfinement approaches in microemulsions are interesting crystallization methods that can target the most thermodynamically stable polymorph in a pharmaceutical system, offering the chance to “leapfrog” Ostwald’s rule of stages. Microemulsion crystallization of glycine, for example, gives the most stable  $\gamma$ -glycine polymorph upon careful control of supersaturation levels.<sup>137</sup> The approach has been applied to

the NSAID painkiller mefenamic acid (MA). When MA is obtained from bulk DMF, it consistently crystallizes in the less stable Form II polymorph regardless of the degree of supersaturation or temperature. However, in DMF microemulsions, the stable Form I is obtained but only at the lowest levels of supersaturation that allow for crystallization. With this method, very low supersaturation levels can be achieved because of the significant reduction in supersaturation that occurs when a nucleus forms within a nanoscale 3D-confined droplet.<sup>138</sup>

Microemulsions have the disadvantage, however, that crystal growth can occur only through droplet merging. Another recently reported method that sidesteps this limitation is the use of structured ternary fluids (STF) comprising octanol, ethanol, and water. The ethanol serves as an amphiphile that is miscible with both the octanol and water, resulting in dynamic nanoscale domains of aqueous and oil regions. As a result, the STFs can serve as environments where nanocrystals can develop and persist for significant durations, leading to improved regulation of crystallization. STF crystallization gives rise to all three ambient pressure polymorphs of glycine (namely, the  $\alpha$ -,  $\gamma$ -, and  $\beta$ -forms), even though the  $\gamma$ -form is typically challenging to crystallize due to its slow growth and the  $\beta$ -form is relatively unstable.<sup>127</sup> Similarly, three metastable polymorphs of ROY, the YN, ON, and R forms, and the stable Y polymorph can all be obtained within a single STF consisting of toluene, isopropyl alcohol, and water.

Nanoconfinement has been applied in CBZ polymorphic form control in a continuous manufacturing context, particularly to produce the less stable CBZ-IV. This is achieved by varying the size of the solution droplets during spray drying. In this controlled procedure, CBZ molecules were enclosed within spray-dried droplets of precise dimensions during the nucleation phase to examine how the limited space within the droplets influences the resulting polymorphic form.<sup>139</sup>

Perhaps one of the most important, environmentally friendly, and versatile modern solid form screening methods is the application of mechanochemical force as in milling or liquid-assisted grinding (LAG).<sup>140,141</sup> Prolonged milling (5 h under neat conditions) gives rise to the recently reported  $\eta$ -form of the very well-studied chlorpropamide,<sup>142</sup> with its structure recently determined by powder diffraction.<sup>119</sup> Surface rugosity has been particularly implicated in the transitions between polymorphs under milling conditions.<sup>142</sup> While no new single-component forms of CBZ have been reported using mechanochemistry, the technique has been used in highly efficient cocrystal screening using a modified planetary mill. CBZ cocrystals were chosen as a model system to benchmark the planetary mill because of their reproducibility, polymorphic and stoichiometric diversity, and the availability of extensive characterization data. This method successfully and efficiently reproduced the expected carbamazepine–saccharin cocrystal. It also revealed a new 1:1 polymorph form of caffeine–maleic acid cocrystal.<sup>143</sup>

Spray drying is also an important technique in novel polymorph discovery, particularly because of the very fast formation of solids from a dispersion. These conditions favor the formation of highly metastable forms. Spray drying has recently resulted in the discovery of the highly metastable  $\zeta$ -form of chlorpropamide, which is calculated to be some 14 kJ mol<sup>-1</sup> less stable than the thermodynamic  $\alpha$ -form, at the limits of the kinds of energies that would be expected to be isolated.<sup>119</sup> A continuous supercritical CO<sub>2</sub> antisolvent-assisted nano spray drying process has been applied to polymorph control in CBZ in which supersaturation conditions occur in a spray drying nozzle in the presence of surfactant additives. This results in the reproducible formation of nanoparticles of the metastable CBZ-t in the presence of sodium stearate, while the stable CBZ-III is obtained with sodium dodecyl sulfate. The fact that the supercritical antisolvent-induced suspension is immediately spray-dried into a fine, dry powder minimizes the chance of any polymorphic transformation. This approach is very different to nonsupersaturated SASD spray drying conditions, which give rise to amorphous CBZ and conventional spray drying methods

without the sc-CO<sub>2</sub> antisolvent which give CBZ-IV.<sup>144</sup> Interestingly, the same surfactant additives also template CBZ-t and CBZ-III, respectively, from sc-CO<sub>2</sub> antisolvent crystallization without spray drying, but on prolonged immersion in the sc-CO<sub>2</sub>/methanol medium CBZ-t showed conversion to CBZ-III.<sup>145</sup>

Finally, solvent vapor annealing of amorphous carbamazepine films has been applied both as a polymorph screening technique and dissolution rate modification method.<sup>146</sup> The spin-coated CBZ film is treated with an atmosphere saturated with molecules of a specific vapor (typically a solvent). These experiments gave rise to four different carbamazepine polymorphs, a solvate and a hydrate, all with spherulitic morphologies. In terms of dissolution behavior, heat-treated amorphous CBZ proved to exhibit immediate release while materials that had been exposed to ethanol released the drug around five times slower. However, even this slower-release material is markedly faster than the conventional powder.

**3.2. The Power of Computationally Led Form Discovery.** Predicting the structure and conditions by which a specific desired solid form can be produced is the holy grail in materials science. In the last 20 years or so, there has been a revolution in the development of computational methods for Crystal Structure Prediction (CSP) and their applications,<sup>147–152</sup> which has truly advanced research in crystal engineering. CBZ, here, has also taught us many lessons.

CSP landscapes of pure CBZ were generated by two independent groups as early as 2006.<sup>112,153</sup> These were the early days for CSP methods. Periodic DFT-d was still not used for modeling molecular crystals; thus, those predictions relied (partially) on the use of force fields. Appropriate modeling of flexibility around the amide functional group of CBZ was found crucial for the prediction of accurate lattice energies in CBZ, with small variations in its pyramidalization impacting the stability of the forms significantly. CBZ forms III and IV were predicted within the low energy structures, CBZ-II was generated with higher lattice energy, and CBZ-I was not predicted due to its high  $Z'$  value. Both CSP studies predicted that structures of CBZ containing catemeric hydrogen-bonded motifs were competitive energetically to the CBZ-III, and thus, further CBZ polymorphs containing catemers should exist. These computational studies inspired a high throughput polymorph screening which, as explained above, led to the previously known CBZ polymorphs III and I as well as CBZ-t and further solvates, all containing H-bonded dimers.<sup>112</sup> In parallel, the crystal structures and hydrogen bonding tendencies of a series of CBZ analogues were explored. These included 10,11-epoxycarbamazepine (ECBZ), 10,11-dihydrocarbamazepine (DHCBZ), and 10-oxcarbazepine (OXCBS).<sup>154</sup> CSP studies on these indicated that a small variation in the molecular shape around the diazepine ring in these CBZ analogues completely switched the H-bonding preferences from dimers to catemers (with DHCBS and OXCBS landscapes dominated by structures containing the catemeric motif). In that same study, seeding of saturated CBZ ethanol solutions with DHCBS forms I and II crystals failed to produce a catemeric polymorph of CBZ.<sup>154</sup>

In separate work, CBZ was cocrystallized with DHCBS resulting in a 1:1 CBZ:DHCBS solid solution containing a catemeric motif and a structure concomitant with that of DHCBS form II (HEMRIB).<sup>155</sup> Recent work in this direction has now shown that solid solution formation can lead to switches in the thermodynamic stabilities of polymorphs, even when the



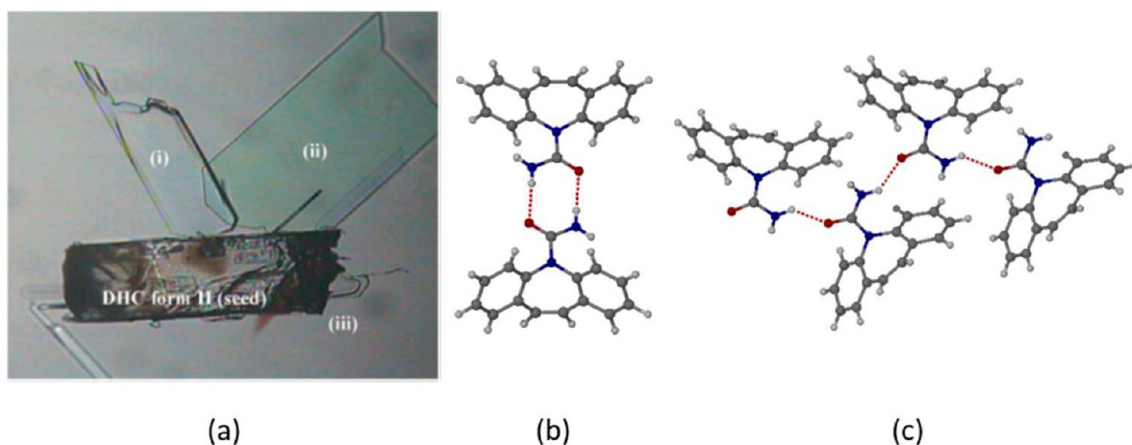


**Figure 13.** (a) A catemeric DHC Form II seed crystal with thin plates (i–iii) of the computationally predicted carbamazepine Form V emerging from the edge faces (reproduced from reference 48 with permission from the Royal Society of Chemistry). (b) Cyclic  $R_2^2(8)$  hydrogen bonded dimer in carbamazepine Forms I–IV. (c) The catemeric CBZ Form V.

guest compound is present in very small amounts.<sup>124,156</sup> Further, seeds of solid solutions have been used to produce yet another polymorph of the infamous compound ROY.<sup>122</sup>

In 2011, after years of further experiments with CBZ, a catemeric polymorph of CBZ (CBZ-V) was finally grown by sublimating CBZ onto a seed crystal of DHCBS-II. Vials containing a DHCBS-II seed suspended above CBZ crystals were sealed and heated to 125 °C for 2 days, resulting in the deposition of CBZ-V onto the DHCBS seed (Figure 13a). Interestingly, CBZ-V crystals grew on the smallest edge face of the seed crystal, while crystals that grew on the copper wire or the walls of the vial were either CBZ-I or III (Figure 13b).<sup>48</sup> CBZ-V, containing the elusive catemeric motif (Figure 13c), was finally realized experimentally after a one-of-a-kind computationally led experimental polymorphic search.

Beyond polymorph prediction, CBZ work also inspired the prediction of inclusion behavior in molecular crystals. One of the early 2006 CSP studies of CBZ correctly generated the structure of CBZ-t, despite the fact that it has an unusually high lattice energy (>8 kJ/mol relative to CBZ-III).<sup>153</sup> This led to further modeling and to the realization (through computation) that CBZ-t could, in fact, become more stable than CBZ-III through further stabilization brought about by the inclusion of guest molecules (such as toluene) in the trigonal pores of the structure. CBZ-t was then crystallized with tridecane in its pores, which evidenced that a larger guest was able to significantly stabilize the CBZ-t structure, remarkably raising its melting point by ~60 °C. Most strikingly, perhaps, was the fact that such a high-energy crystal structure with pores was generated by CSP of CBZ alone, without the need of modeling the guest so crucial for its observation. This realization led to further research in which it was shown that a great variety of inclusion frameworks (including those seen in urea inclusion compounds) could be generated computationally with CSP of the host alone. A protocol was developed for the prediction of structures of porous inclusion frameworks where CSP followed by a ranking based on a combination of lattice energy and available volume for guest inclusion was used to identify inclusion structures of potential experimental realization.<sup>157</sup> Years later, this strategy led to the discovery of novel porous molecular materials,<sup>158</sup> and the prediction of the ability of compounds to form inclusion solvates<sup>159</sup> and hydrates.<sup>160</sup>

CBZ also led the way in the computational prediction of solvates. The first crystal structure prediction study of an acetic acid solvate was performed on CBZ and its close analogue DHCBS in 2006. CSP of multicomponent systems, although more routine today, was challenging at the time because of the greater number of independent variables that require exploration. Although there was some pioneering CSP prior work on a handful of other multicomponent systems,<sup>161–163</sup> this CBZ and DHCBS study was the first to predict the formation and structure of an acetic acid solvate prior to any experimentation. This work on solvates led to further studies and the realization that CSP landscapes can also anticipate the possibility of structural disorder in crystal structures. In 2011, a CSP landscape of 1:1 CBZ:DMSO revealed that two of the low-energy predicted solvate structures were identical for the CBZ occupancy but had the DMSO oriented in two different ways.<sup>31</sup> A computational combination of these two and molecular dynamic (MD) simulations then showed that indeed the experimental structure must be a combination of these two ideal structures, showing disorder. The MD simulations showed that, while this disorder is static at low temperatures, it becomes dynamic at higher temperatures, with the DMSO molecule able to reorient itself in the structure through a simple rotation.<sup>31</sup>

While there remain many frontiers and challenges to be addressed in crystal structure prediction,<sup>151</sup> the lessons learned on these by CBZ have been remarkable and historically important. Solid forms can vary in  $Z'$  and in composition, can contain disorder and flexibility of high complexity, and thus there is almost an infinite universe of solid forms to be explored both experimentally and computationally. While significant advances have been achieved in some of these areas of CSP including prediction of stoichiometry,<sup>164,165</sup> hydration,<sup>152,166</sup> accurate modeling of conformational energies,<sup>167</sup> or reduction of overpredicted structures,<sup>168,169</sup> we are yet to understand and establish further links between the structures generated in the computer and those that can be crystallized experimentally.<sup>170,171</sup> The work on CBZ has illustrated, beyond any other work, how experimental and computational synergy is a must for the crystal engineering work of the future.

**3.3. Conversions between CBZ-DH, Anhydrous Forms and Amorphous.** Understanding form conversion and ranges of solid form stabilities is key for crystal engineering and pharmaceutical materials sciences. Especially, conversions



between neat crystalline solids, amorphous, and hydrate forms need to be well understood prior to drug formulation.

The mechanism of dehydration of CBZ-DH powders (and the forms it leads to) is heavily influenced by the conditions of dehydration used including temperature and relative humidity (RH).<sup>172,173</sup> At room temperature and 0% RH, CBZ-DH converts to CBZ-A.<sup>56,174</sup> At room temperature and ~10% RH, CBZ-DH converts to CBZ-I, and at RHs above that into a mixture of CBZ-I and CBZ-III. Dehydration above the  $T_g$  leads to mixtures of CBZ-IV and -I, with CBZ-I becoming the sole form above 100 °C.<sup>56</sup> Kachrimanis and Griesser established that the CBZ-DH process occurs in two overlapping steps of different kinetics and is influenced by the environment: (i) first the dehydration of the weaker water bound to the carbonyl of carbonyl group CBZ and (ii) second the dehydration of the second more strongly bound water bound to the  $NH_2$  of CBZ. Removal of the first water leads to amorphization and of the second water to crystallization of either CBZ-IV or CBZ-I.<sup>56</sup>

In solution, both conversions from and to the CBZ-DH have been investigated. For the solvent-mediated conversions of CBZ-III and CBZ-I into CBZ-DH in aqueous suspensions, it was found that the morphology of the anhydrous form used had a greater impact on the kinetics of the conversion than the polymorphic form used.<sup>175</sup> Further work then highlighted that the kinetics of the conversion could be greatly accelerated by increasing the stirring, thus promoting grinding conditions. Milling changed the rate-controlling step of the process from the crystallization of CBZ-DH to the dissolution of CBZ-A produced by milling.<sup>176</sup> These works showed the important role played by surfaces in enabling the nucleation of the CBZ-DH with the availability of CBZ-A accelerating these kinetics.

**3.4. Beyond the Crystal.** Solid-state NMR spectroscopy as well as X-ray scattering studies combined with the Empirical Potential Structure Refinement of liquid and amorphous CBZ has led to a further understanding of the binding modes of CBZ in environments other than the crystalline solid state. In melted-liquid CBZ, the aromatic stacking interactions of the butterfly rings dominate, with the number of H-bonds significantly increasing upon formation of the glassy state. The lack of crystal symmetry in the glassy state results in the formation of H-bond structures other than dimers, including trimers and tetramers not observed in the crystalline state.<sup>177</sup> In line with this, studies of CBZ deposited on Au(111) surfaces by scanning tunneling microscopy (STM) showed the assembly of CBZ into stable tetramers through H-bonding (Figure 14), these, in turn, assembling through aromatic sandwich interactions. Remarkably, electrospray ionization mass spectra of CBZ show an intense peak corresponding to the mass of a tetramer, suggesting that a four-molecule cluster has significant stability even in the gas phase.<sup>178</sup>

**3.5. The Power of Crystal Engineering to Influence Solid-State Properties.** Sections 2.8 and 2.9 illustrate the variety of neutral and ionic cocrystals formed by CBZ and their highly varied properties. The formation of over 60 cocrystals by CBZ, partly as a result of its unusual combination of molecular structural features, shows the tremendous power of crystal engineering approaches to modify solid-state properties. Section 3.3 also shows that amorphous CBZ is accessible by dehydration, and as a low solubility (BCS class II) drug, solid forms of compounds like CBZ with potentially higher solubility are of interest in improving oral bioavailability. Like many amorphous forms, CBZ-A can suffer from issues of physical or chemical instability. CBZ-A, surprisingly, does not give a

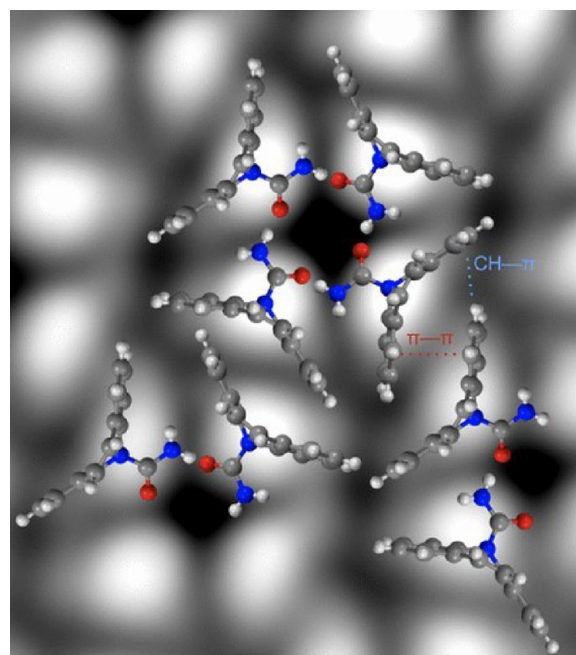


**Figure 14.** STM image of an ordered array of CBZ hydrogen bonded tetramers deposited on Au(111). Reproduced from reference 178. Copyright 2020 American Chemical Society.

supersaturated solution in gastric media and, in fact, the solution concentration proves lower than that obtained from crystalline CBZ-III because of rapid conversion to the insoluble dihydrate. The use of polymers such as PVP and HMPC to stabilize the amorphous form also did not result in any enhanced solubility with a similar initial concentration to the crystalline form, dropping after just over an hour again because of the formation of dihydrate.<sup>179</sup> Instead of polymers, small molecule coamorphous materials have also been made with CBZ.<sup>35</sup> CBZ forms a coamorphous 1:1 material with citric acid by ball milling. However, like many coamorphous substances, it exhibits a relatively low glass transition temperature ( $T_g$ ) in comparison to polymeric solid dispersions. The low  $T_g$  of 39 °C in combination with hygroscopicity results in the transformation to a supercooled melt under ambient conditions. This issue could be addressed by salt formation with L-arginine to give ternary coamorphous blends with  $T_g$  ranging from 77 to 128 °C depending on the amount of arginine.<sup>35</sup> CBZ is also one of several drugs that form binary coamorphous phases with the relatively unusual *N*-vinylcaprolactam dimer cofomer, which has strong hydrogen bond acceptor properties but little donor acidity. CBZ forms a stable coamorphous phase by comelting. While the  $T_g$  is close to room temperature, the material remains amorphous even at a 2:1 CBZ to conformer ratio over several days before slowly crystallizing over 4 weeks.<sup>180</sup>

CBZ, like many small molecules, can potentially form inclusion complexes with carriers such as cyclodextrins, and the entrapment of the drug within the hollow carrier can dramatically influence the material's properties. While there does not appear to be a report of crystal structure data, phase-solubility studies have shown that soluble CBZ complexes form with  $\alpha$ -,  $\beta$ -, and hydroxypropyl cyclodextrins, while the  $\gamma$ -cyclodextrin ( $\gamma$ -CD) complex is insoluble. The hydroxypropyl-cyclodextrin complex gives rise to the highest apparent solubility.<sup>181</sup> Complexation by cyclodextrins can potentially be used as an efficient drug delivery mechanism. CBZ has been

found to enter the shell of core–shell cholesteryl oleate (ChO)/ $\gamma$ -CD nanoparticles as a crystalline nanosheet  $\gamma$ -CD inclusion complex. Interestingly the channel inclusion structure of CBZ-t can also be used to form CBZ–polymer inclusion complexes in which the CBZ is the host rather than the guest. Both hydrophilic poly(ethylene glycol) and hydrophobic poly(3-caprolactone) are included and have the CBZ-t channel crystal structure. Compared to CBZ-t, the poly(ethylene glycol) complex has a faster dissolution rate under both sink and nonsink conditions while the poly(3-caprolactone) complex proved to be more stable than CBZ-t with respect to transformation to other crystalline CBZ forms.<sup>33,34</sup>

Finally, the probing of mechanical behavior and the link between mechanical properties and the structure of crystals is an exciting area of research in Crystal Engineering.<sup>182</sup> In the past decade or so, pharmaceutical crystals have been probed by the technique of nanoindentation,<sup>182–185</sup> which has allowed for the exploration of links between structure–mechanical properties. This has allowed for the development of design rules for making flexible crystals,<sup>186</sup> the use of cocrystallization and polymorphism to improve mechanical behavior,<sup>187–189</sup> or the understanding of the coexistence of elastic and plastic bending<sup>190</sup> to name a few. In this context, CBZ-III has also been studied with nanoindentation.<sup>191</sup> Interestingly, the mechanical behavior of CBZ-III was found to be highly anisotropic with the {020} faces found to be nearly 30% stiffer than the {002} and the {101} faces. Modeling of the system highlighted the importance of molecular flexibility for mechanical behavior. The breathing of the butterfly ring in CBZ was found to contribute to a softening of the mechanical behavior in CBZ-III.<sup>191</sup>

**3.6. Remediating the Environmental Legacy of Modern Pharmaceuticals.** One final lesson that we can learn from CBZ is that it is one of the most common of many persistent, stable pharmaceuticals and personal care products (PPCPs) that are beginning to accumulate in the environment as a result of humanity's extensive reliance on modern medicines.<sup>192</sup> CBZ is particularly commonly observed in food crops that have been grown on soil irrigated with treated sewage effluent, indicating current treatment methodologies do not degrade CBZ. Since drugs such as CBZ are by definition biologically active, increasing accumulation of pharmaceuticals in the biosphere is potentially a cause of unwanted consequences, and there is a role for solid-state science in ameliorating this growing potential problem. While typically organic pollutants are broken down using biochemical processes, these may be slow and ineffective under certain conditions such as high salinity. One approach is to take advantage of mechanochemical activation to activate the breakdown of CBZ by active inorganic surfaces. Sorption of CBZ onto Al-montmorillonite clay results in enhanced degradation; however, ball milling with magnetite has been found to result in complete degradation of BCZ to iminostilbene. There is something of a symmetry between mechanochemical approaches to prepare CBZ cocrystals and similar ways to address its destruction.<sup>130</sup> Other approaches to CBZ removal have involved molecularly imprinted polymers (MIPs) with an optimized MIP based on vinylbenzoic acid adsorbing 28 mg g<sup>-1</sup> of CBZ. Selective adsorption arises from a combination of just the interactions found in CBZ solid forms, namely hydrogen bonding, aromatic interactions, and van der Waals forces.<sup>193</sup> The use of activated carbon and biochar are also

important approaches that are the subject of ongoing research.<sup>194</sup>

## 4. CONCLUSION

Carbamazepine is highly polymorphic and is one of the most prolific formers of multicomponent crystals known. Certainly, its awkward shape, hydrogen bond donor and acceptor ability, mismatch of the number of donors and acceptors, aromatic stacking characteristics, and basicity contribute significantly to this propensity. However, it is also the amount of time and resources that have been spent on the compound that has revealed much of its rich solid-state behavior. The rigidity of CBZ makes it relatively tractable from a CSP perspective, and this, in turn, has led to careful, unusual experiments to test predictions such as the seeded discovery of the predicted neat form V. As more has become known about the compound, it has increasingly been used as a model system for the exploration of new methodologies. The fact that as recently as 2022 another single-component polymorph has been revealed suggests that extensive study of many such drug molecules will continue to increase our knowledge of their solid form diversity. The recent explosion in novel crystallization and solid form discovery methods is at once a blessing and a curse. While ever more materials are becoming experimentally accessible, the effort and resources required to search for them are increasingly significant. This means that computationally guided experiments in conjunction with data-based approaches are now hugely important. It is truly remarkable what such techniques have revealed about just the one example of CBZ, and this diversity highlights McCrone's foresight in speculating that the number of polymorphs discovered for a given compound is proportional to the amount of time and money spent on it.

## ■ AUTHOR INFORMATION

### Corresponding Authors

Amy V. Hall – Department of Chemistry, Durham DH1 3LE, U.K.; [orcid.org/0000-0002-3664-9229](https://orcid.org/0000-0002-3664-9229);  
Email: [amy.v.hall@durham.ac.uk](mailto:amy.v.hall@durham.ac.uk)

Aurora J. Cruz-Cabeza – Department of Chemistry, Durham DH1 3LE, U.K.; [orcid.org/0000-0002-0957-4823](https://orcid.org/0000-0002-0957-4823);  
Email: [aurora.j.cruz-cabeza@durham.ac.uk](mailto:aurora.j.cruz-cabeza@durham.ac.uk)

Jonathan W. Steed – Department of Chemistry, Durham DH1 3LE, U.K.; [orcid.org/0000-0002-7466-7794](https://orcid.org/0000-0002-7466-7794);  
Email: [jon.steed@durham.ac.uk](mailto:jon.steed@durham.ac.uk)

Complete contact information is available at:  
<https://pubs.acs.org/10.1021/acs.cgd.4c00555>

### Notes

The authors declare no competing financial interest.



## Biographies



From left to right: Aurora J. Cruz-Cabeza, Amy V. Hall, and Jonathan W. Steed.

Amy V. Hall was born in Nottinghamshire, UK, a few miles away from Sherwood Forest, famous for hosting Robin Hood and his band of Merry Men. As Amy comes from a strong working-class family of ex-coal miners, she was the first of her family to study at university. Amy obtained her BSc in Pharmaceutical Science at the University of Lincoln in 2017, and from there, she was propelled into a PhD in Chemistry at Durham University studying radiation-sensitive cocrystals and salts. Amy completed her doctorate in 2020 and decided she enjoyed research in Durham so much, that she continued in the department as a Postdoc, working to improve the physicochemical properties of leishmaniasis drugs. Amy established her group at Durham in 2023 and is currently a Leverhulme Trust Early Career Fellow, with her research interests focusing on the crystal engineering of pharmaceutical solid forms. Outside of the realm of science, Amy loves being a Mum to an energetic toddler and Springer Spaniel, as well as baking and listening to 2000s pop classics. She also appreciates the beauty of North East England and willingly embraces the rain.

Aurora J. Cruz-Cabeza was born in Jaén, one of the most beautiful cities in Spain. She was fascinated by the world from an early age with a particular love for stars and music. She bought her first guitar at the age of 11 and her first telescope at the age of 15. Aurora wanted to study astrophysics but was unable to do so due to practical limitations. As such, she decided to move her passion for the big for a passion for the small and studied Physical Chemistry instead. She completed two BSc simultaneously, one in Physical Chemistry and a second one in Music, with classical guitar as instrument. After earning a Master's in heterogeneous catalysis, she moved to the University of Cambridge (UK) where she earned a PhD in the study of molecular crystals. At Cambridge, Aurora was the guitarist and second lead voice in a band called "Los Elementos"—all its members being chemists—and they played in numerous May Balls around Cambridge through the years as well as in events in the Chemistry Department. In the following eight years, Aurora took several scientific jobs in the UK, The Netherlands, and Switzerland and was presented with the greatest scientific challenge of it all: being a mum whilst trying to follow an academic career and continue to play music. Aurora then moved to Manchester where she started her independent academic career in Chemical Engineering. In 2022, she moved to Durham as a Professor of Materials Chemistry. Aurora's office is decorated with a nice collection of guitars and ukuleles and is always opened to her students and colleagues. She has won numerous prizes and published many interesting scientific papers. She is indebted to the wonderful people she has had the pleasure to work with during her career, her amazing friends, and a supportive family.

Like most people, Jon Steed was born. In his case, it happened in Wimbledon, just in time for the first moon landing. In 1987, he went to University College London to make his fortune and ended up staying for a very enjoyable PhD with Derek Tocher in which he made a lot of ruthenium compounds for some reason. He who is tired of London is tired of life, so the saying goes. But, nevertheless in 1993 Jon went to the University of Alabama for a Postdoc with Jerry Atwood. There he learned about Supramolecular Chemistry, College Football, and Parties. It was quite a change! As a result, two years later, Jon had to leave the country quickly and returned to London taking a lectureship at King's College. This is suspected to be an indirect cause of the subsequent, fortunately temporary, closure of King's Chemistry Department. In 2004, he joined Durham University, where he has been ever since. He has won several goody bags from the Royal Society of Chemistry and each time immediately changes research area. These days he really likes pharmaceutical crystals and gels, although he usually does not know what the drug actually does. Despite this ignorance, he writes a lot of papers and books about Supramolecular Chemistry as well as editing *Crystal Growth & Design*. He very much enjoys bicycles, gardening, and watching students and co-workers rapidly come to know more than he does.

## REFERENCES

- (1) Braga, D. Crystal engineering: from promise to delivery. *Chem. Commun.* **2023**, *59*, 14052–14062.
- (2) Price, S. L. Predicting crystal structures of organic compounds. *Chem. Soc. Rev.* **2014**, *43*, 2098–2111.
- (3) Reilly, A. M.; Cooper, R. I.; Adjiman, C. S.; Bhattacharya, S.; Boese, A. D.; Brandenburg, J. G.; Bygrave, P. J.; Bylisma, R.; Campbell, J. E.; Car, R.; Case, D. H.; Chadha, R.; Cole, J. C.; Cosburn, K.; Cuppen, H. M.; Curtis, F.; Day, G. M.; DiStasio Jr, R. A.; Dzyabchenko, A.; van Eijck, B. P.; Elking, D. M.; van den Ende, J. A.; Facelli, J. C.; Ferraro, M. B.; Fusti-Molnar, L.; Gatsiou, C.-A.; Gee, T. S.; de Gelder, R.; Ghiringhelli, L. M.; Goto, H.; Grimme, S.; Guo, R.; Hofmann, D. W. M.; Hoja, J.; Hylton, R. K.; Iuzzolino, L.; Jankiewicz, W.; de Jong, D. T.; Kendrick, J.; de Klerk, N. J. J.; Ko, H.-Y.; Kuleshova, L. N.; Li, X.; Lohani, S.; Leusen, F. J. J.; Lund, A. M.; Lv, J.; Ma, Y.; Marom, N.; Masunov, A. E.; McCabe, P.; McMahon, D. P.; Meekes, H.; Metz, M. P.; Misquitta, A. J.; Mohamed, S.; Monserrat, B.; Needs, R. J.; Neumann, M. A.; Nyman, J.; Obata, S.; Oberhofer, H.; Oganov, A. R.; Orendt, A. M.; Pagola, G. I.; Pantelides, C. C.; Pickard, C. J.; Podeszwa, R.; Price, L. S.; Price, S. L.; Pulido, A.; Read, M. G.; Reuter, K.; Schneider, E.; Schober, C.; Shields, G. P.; Singh, P.; Sugden, I. J.; Szalewicz, K.; Taylor, C. R.; Tkatchenko, A.; Tuckerman, M. E.; Vacarro, F.; Vasileiadis, M.; Vazquez-Mayagoitia, A.; Vogt, L.; Wang, Y.; Watson, R. E.; de Wijs, G. A.; Yang, J.; Zhu, Q.; Groom, C. R. Report on the sixth blind test of organic crystal structure prediction methods. *Acta Crystallogr., Sect. B: Struct. Sci., Cryst. Eng. Mater.* **2016**, *72*, 439–459.
- (4) Cruz-Cabeza, A. J.; Feeder, N.; Davey, R. J. Open questions in organic crystal polymorphism. *Commun. Chem.* **2020**, *3* (1), 4.
- (5) Cruz-Cabeza, A. J.; Reutzel-Edens, S. M.; Bernstein, J. Facts and fictions about polymorphism. *Chem. Soc. Rev.* **2015**, *44*, 8619–8635.
- (6) Tolou-Ghamari, Z.; Zare, M.; Habibabadi, J. M.; Najafi, M. R. A quick review of carbamazepine pharmacokinetics in epilepsy from 1953 to 2012. *J. Res. Med. Sci.* **2013**, *18*, S81–S85.
- (7) Groom, C. R.; Bruno, I. J.; Lightfoot, M. P.; Ward, S. C. The Cambridge Structural Database. *Acta Crystallogr., Sect. B: Struct. Sci., Cryst. Eng. Mater.* **2016**, *72*, 171–179.
- (8) Aitipamula, S.; Banerjee, R.; Bansal, A. K.; Biradha, K.; Cheney, M. L.; Choudhury, A. R.; Desiraju, G. R.; Dikundwar, A. G.; Dubey, R.; Duggirala, N.; Ghogale, P. P.; Ghosh, S.; Goswami, P. K.; Goud, N. R.; Jetti, R.; Karpinski, P.; Kaushik, P.; Kumar, D.; Kumar, V.; Moulton, B.; Mukherjee, A.; Mukherjee, G.; Myerson, A. S.; Puri, V.; Ramanan, A.; Rajamannar, T.; Reddy, C. M.; Rodriguez-Hornedo, N.; Rogers, R. D.; Row, T. N. G.; Sanphui, P.; Shan, N.; Shete, G.; Singh, A.; Sun, C. Q. C.;



- Swift, J. A.; Thaimattam, R.; Thakur, T. S.; Thaper, R. K.; Thomas, S. P.; Tothadi, S.; Vangala, V. R.; Variankaval, N.; Vishweshwar, P.; Weyna, D. R.; Zaworotko, M. J. Polymorphs, Salts, and Cocrystals: What's in a Name? *Cryst. Growth Des.* **2012**, *12*, 2147–2152.
- (9) Childs, S. L.; Wood, P. A.; Rodriguez-Hornedo, N.; Reddy, L. S.; Hardcastle, K. I. Analysis of 50 Crystal Structures Containing Carbamazepine Using the Materials Module of Mercury CSD. *Cryst. Growth Des.* **2009**, *9*, 1869–1888.
- (10) Buist, A. R.; Kennedy, A. R. Ionic Cocrystals of Pharmaceutical Compounds: Sodium Complexes of Carbamazepine. *Cryst. Growth Des.* **2014**, *14*, 6508–6513.
- (11) Buist, A. R.; Edgeley, D. S.; Kabova, E. A.; Kennedy, A. R.; Hooper, D.; Rollo, D. G.; Shankland, K.; Spillman, M. J. Salt and Ionic Cocrystalline Forms of Amides: Protonation of Carbamazepine in Aqueous Media. *Cryst. Growth Des.* **2015**, *15*, 5955–5962.
- (12) Bolla, G.; Sarma, B.; Nangia, A. K. Crystal Engineering of Pharmaceutical Cocrystals in the Discovery and Development of Improved Drugs. *Chem. Rev.* **2022**, *122*, 11514–11603.
- (13) Drozd, K. V.; Manin, A. N.; Churakov, A. V.; Perlovich, G. L. Novel drug-drug cocrystals of carbamazepine with para-aminosalicylic acid: screening, crystal structures and comparative study of carbamazepine cocrystal formation thermodynamics. *CrystEngComm* **2017**, *19*, 4273–4286.
- (14) Devogelaer, J. J.; Meeke, H.; Tinnemans, P.; Vlieg, E.; de Gelder, R. Co-crystal Prediction by Artificial Neural Networks. *Angew. Chem., Int. Ed.* **2020**, *59*, 21711–21718.
- (15) Vishweshwar, P.; McMahon, J. A.; Oliveira, M.; Peterson, M. L.; Zaworotko, M. J. The predictably elusive form II of aspirin. *J. Am. Chem. Soc.* **2005**, *127*, 16802–16803.
- (16) Aitipamula, S.; Chow, P. S.; Tan, R. B. H. Structural, Spectroscopic and Thermal Analysis of Cocrystals of Carbamazepine and Piracetam with Hydroquinone. *J. Chem. Crystallogr.* **2011**, *41*, 1604–1611.
- (17) Du, J. J.; Stanton, S. A.; Fakhri, S.; Hawkins, B. A.; Williams, P. A.; Groundwater, P. W.; Overgaard, J.; Platts, J. A.; Hibbs, D. E. Exploring the Solubility of the Carbamazepine-Saccharin Cocrystal: A Charge Density Study. *Cryst. Growth Des.* **2021**, *21*, 4259–4275.
- (18) Horstman, E. M.; Goyal, S.; Pawate, A.; Lee, G.; Zhang, G. G. Z.; Gong, Y. C.; Kenis, P. J. A. Crystallization Optimization of Pharmaceutical Solid Forms with X-ray Compatible Microfluidic Platforms. *Cryst. Growth Des.* **2015**, *15*, 1201–1209.
- (19) Schneider-Rauber, G.; Bond, A. D.; Ho, R.; Nere, N.; Bordawekar, S.; Sheikh, A. Y.; Jones, W. Effect of Solution Composition on the Crystallization of Multicomponent Forms of Carbamazepine beyond Crystal Form and Shape: Surface as a Source of Diversity in the Solid-Form Landscape. *Cryst. Growth Des.* **2021**, *21*, 52–64.
- (20) Roca-Paixao, L.; Correia, N. T.; Danede, F.; Guerain, M.; Affouard, F. Carbamazepine/Tartaric Acid Cocrystalline Forms: When Stoichiometry and Synthesis Method Matter. *Cryst. Growth Des.* **2023**, *23*, 1355.
- (21) Fischer, F.; Joester, M.; Rademann, K.; Emmerling, F. Survival of the Fittest: Competitive Co-crystal Reactions in the Ball Mill. *Chem.—Eur. J.* **2015**, *21*, 14969–14974.
- (22) Inoue, Y.; Sato, S.; Yamamoto, C.; Yamasaki, M.; Kanamoto, I. Study of Complex Formation of Carbamazepine with Thiourea. *Chem. Pharm. Bull.* **2014**, *62*, 1125–1130.
- (23) Babu, N. J.; Reddy, L. S.; Nangia, A. Amide-N-oxide heterosynthons and amide dimer homosynthons in cocrystals of carboxamide drugs and pyridine N-oxides. *Mol. Pharmaceutics* **2007**, *4*, 417–434.
- (24) McMahon, J. A.; Bis, J. A.; Vishweshwar, P.; Shattock, T. R.; McLaughlin, O. L.; Zaworotko, M. J. Crystal engineering of the composition of pharmaceutical phases. 3. Primary amide supra-molecular heterosynthons and their role in the design of pharmaceutical co-crystals. *Z. Kristallogr. - Cryst. Mater.* **2005**, *220*, 340–350.
- (25) Jayasankar, A.; Reddy, L. S.; Bethune, S. J.; Rodriguez-Hornedo, N. Role of Cocrystal and Solution Chemistry on the Formation and Stability of Cocrystals with Different Stoichiometry. *Cryst. Growth Des.* **2009**, *9*, 889–897.
- (26) Corpinot, M. K.; Guo, R.; Tocher, D. A.; Buanz, A. B. M.; Gaisford, S.; Price, S. L.; Bucar, D. K. Are Oxygen and Sulfur Atoms Structurally Equivalent in Organic Crystals? *Cryst. Growth Des.* **2017**, *17*, 827–833.
- (27) Prohens, R.; Font-Bardia, M.; Barbas, R. Water wires in the nanoporous form II of carbamazepine: a single-crystal X-ray diffraction analysis. *CrystEngComm* **2013**, *15*, 845–847.
- (28) Harris, R. K.; Ghi, P. Y.; Puschmann, H.; Apperley, D. C.; Griesser, U. J.; Hammond, R. B.; Ma, C. Y.; Roberts, K. J.; Pearce, G. J.; Yates, J. R.; Pickard, C. J. Structural studies of the polymorphs of carbamazepine, its dihydrate, and two solvates. *Org. Process Res. Dev.* **2005**, *9*, 902–910.
- (29) Fleischman, S. G.; Kuduva, S. S.; McMahon, J. A.; Moulton, B.; Walsh, R. D. B.; Rodriguez-Hornedo, N.; Zaworotko, M. J. Crystal engineering of the composition of pharmaceutical phases: Multiple-component crystalline solids involving carbamazepine. *Cryst. Growth Des.* **2003**, *3*, 909–919.
- (30) Schneider-Rauber, G.; Arhangelskis, M.; Bond, A. D.; Ho, R.; Nere, N.; Bordawekar, S.; Sheikh, A. Y.; Jones, W. Polymorphism and surface diversity arising from stress-induced transformations - the case of multi-component forms of carbamazepine. *Acta Crystallogr., Sect. B: Struct. Sci., Cryst. Eng. Mater.* **2021**, *77*, 54–67.
- (31) Cruz-Cabeza, A. J.; Day, G. M.; Jones, W. Structure prediction, disorder and dynamics in a DMSO solvate of carbamazepine. *Phys. Chem. Chem. Phys.* **2011**, *13*, 12808–12816.
- (32) Cruz-Cabeza, A. J.; Day, G. M.; Motherwell, W. D. S.; Jones, W. Prediction and observation of isostructurality induced by solvent incorporation in multicomponent crystals. *J. Am. Chem. Soc.* **2006**, *128*, 14466–14467.
- (33) Ishimoto, A.; Sasako, H.; Omori, M.; Higashi, K.; Ueda, K.; Koyama, K.; Moribe, K. Drug-Loaded Nanocarriers Composed of Cholesterol Oleate Crystal Cores and Multiple-Nanosheet Shells of  $\beta$ -Cyclodextrin Inclusion Complex Crystals. *Langmuir* **2022**, *38*, 10454–10464.
- (34) Chen, L.; Huang, Y. B. The guest polymer effect on the dissolution of drug-polymer crystalline inclusion complexes. *RSC Adv.* **2021**, *11*, 13091–13096.
- (35) Ueda, H.; Wu, W. Q.; Löbmann, K.; Grohgan, H.; Müllertz, A.; Rades, T. Application of a Salt Cofomer in a Co-Amorphous Drug System Dramatically Enhances the Glass Transition Temperature: A Case Study of the Ternary System Carbamazepine, Citric Acid, and L-Arginine. *Mol. Pharmaceutics* **2018**, *15*, 2036–2044.
- (36) ChemAxon, Marvin (version 23.16), [www.chemaxon.com](http://www.chemaxon.com), (accessed December 13, 2023).
- (37) McCrone, W. C. In *Polymorphism in Physics and Chemistry of the Organic Solid State*, Fox, D.; Labes, M. M.; Weissberger, A., Eds.; Wiley Interscience: New York, 1965, Vol. 2, pp 725–767.
- (38) Li, Z.; Matzger, A. J. Influence of Cofomer Stoichiometric Ratio on Pharmaceutical Cocrystal Dissolution: Three Cocrystals of Carbamazepine/4-Aminobenzoic Acid. *Mol. Pharmaceutics* **2016**, *13*, 990–995.
- (39) Cruz-Cabeza, A. J.; Lusi, M.; Wheatcroft, H. P.; Bond, A. D. The role of solvation in proton transfer reactions: implications for predicting salt/co-crystal formation using the  $\Delta p < i > K < /i > < sub > a < /sub > > rule$ . *Faraday Discuss.* **2022**, *235*, 446–466.
- (40) Li, Y. H.; Han, J.; Zhang, G. G. Z.; Grant, D. J. W.; Suryanarayanan, R. In situ dehydration of carbamazepine dihydrate: A novel technique to prepare amorphous anhydrous carbamazepine. *Pharm. Dev. Technol.* **2000**, *5*, 257–266.
- (41) Asare-Addo, K.; Adebisi, A. O.; Ghori, M. U. Co-amorphous drug systems of carbamazepine: intrinsic dissolution rate improvements. *Int. J. Basic Med. Sci. Pharm.* **2016**, *6*, 42–46.
- (42) Seefeldt, K.; Miller, J.; Alvarez-Nunez, F.; Rodriguez-Hornedo, N. Crystallization pathways and kinetics of carbamazepine-nicotinamide cocrystals from the amorphous state by in situ thermomicroscopy, spectroscopy and calorimetry studies. *J. Pharm. Sci.* **2007**, *96*, 1147–1158.
- (43) Wu, W. Q.; Wang, Y. X.; Lobmann, K.; Grohgan, H.; Rades, T. Transformations between Co-Amorphous and Co-Crystal Systems and

Their Influence on the Formation and Physical Stability of Co-Amorphous Systems. *Mol. Pharmaceutics* **2019**, *16*, 1294–1304.

(44) Grzesiak, A. L.; Lang, M. D.; Kim, K.; Matzger, A. J. Comparison of the four anhydrous polymorphs of carbamazepine and the crystal structure of form I. *J. Pharm. Sci.* **2003**, *92*, 2260–2271.

(45) Lowes, M. M. J.; Cairn, M. R.; Lotter, A. P.; Vanderwatt, J. G. PHYSICO-CHEMICAL PROPERTIES AND X-RAY STRUCTURAL STUDIES OF THE TRIGONAL POLYMORPH OF CARBAMAZEPINE. *J. Pharm. Sci.* **1987**, *76*, 744–752.

(46) Cruz-Cabeza, A. J.; Day, G. M.; Motherwell, W. D. S.; Jones, W. Solvent inclusion in form II carbamazepine. *Chem. Commun.* **2007**, 1600–1602.

(47) Fabbiani, F. P. A.; Byrne, L. T.; McKinnon, J. J.; Spackman, M. A. Solvent inclusion in the structural voids of form II carbamazepine: single-crystal X-ray diffraction, NMR spectroscopy and Hirshfeld surface analysis. *CrystEngComm* **2007**, *9*, 728–731.

(48) Arlin, J. B.; Price, L. S.; Price, S. L.; Florence, A. J. A strategy for producing predicted polymorphs: catemeric carbamazepine form V. *Chem. Commun.* **2011**, *47*, 7074–7076.

(49) Fellah, N.; Tahsin, L.; Zhang, C. J.; Kahr, B.; Ward, M. D.; Shtukenberg, A. G. Efficient Polymorph Screening through Crystallization from Bulk and Confined Melts. *Cryst. Growth Des.* **2022**, *22*, 7527–7543.

(50) Reboul, J.; Cristau, B.; Soyfer, J.; Astier, J. 5 H -Dibenz [ b, f ]azépinecarboxamide-5 (carbamazépine). *Acta Crystallogr.* **1981**, *B37*, 1844–1848.

(51) Lang, M. D.; Kampf, J. W.; Matzger, A. J. Form IV of carbamazepine. *J. Pharm. Sci.* **2002**, *91*, 1186–1190.

(52) Kuhnert-Brandstatter, M.; Kofler, A.; Vlachopoulos, A. Beitrag zur mikroskopischen Charakterisierung und Identifizierung von Arzneimitteln unter Einbeziehung der UV-Spektrophotometrie. *Sci. Pharm.* **1968**, *36*, 164–179.

(53) Behme, R. J.; Brooke, D. HEAT OF FUSION MEASUREMENT OF A LOW MELTING POLYMORPH OF CARBAMAZEPINE THAT UNDERGOES MULTIPLE-PHASE CHANGES DURING DIFFERENTIAL SCANNING CALORIMETRY ANALYSIS. *J. Pharm. Sci.* **1991**, *80*, 986–990.

(54) Lisgarten, J. N.; Palmer, R. A.; Saldanha, J. W. CRYSTAL AND MOLECULAR-STRUCTURE OF 5-CARBAMYL-SH-DIBENZO B, F AZEPINE. *J. Crystallogr. Spectrosc. Res.* **1989**, *19*, 641–649.

(55) Krahn, F. U.; Mielck, J. B. RELATIONS BETWEEN SEVERAL POLYMORPHIC FORMS AND THE DIHYDRATE OF CARBAMAZEPINE. *Pharm. Acta Helv.* **1987**, *62*, 247–254.

(56) Kachrimanis, K.; Griesser, U. J. Dehydration Kinetics and Crystal Water Dynamics of Carbamazepine Dihydrate. *Pharm. Res.* **2012**, *29*, 1143–1157.

(57) Zheltikova, D.; Losev, E.; Boldyreva, E. To touch or not to touch? Fingerprint-assisted grinding of carbamazepine form III. *CrystEngComm* **2023**, *25*, 4879–4888.

(58) Broadhurst, E. T.; Xu, H.; Parsons, S.; Nudelman, F. Revealing the early stages of carbamazepine crystallization by cryoTEM and 3D electron diffraction. *IUCr.* **2021**, *8*, 860–866.

(59) Kobayashi, Y.; Ito, S.; Itai, S.; Yamamoto, K. Physicochemical properties and bioavailability of carbamazepine polymorphs and dihydrate. *Int. J. Pharm.* **2000**, *193*, 137–146.

(60) Fateixa, S.; Nogueira, H. I. S.; Paixao, J. A.; Fausto, R.; Trindade, T. Insightful vibrational imaging study on the hydration mechanism of carbamazepine. *Phys. Chem. Chem. Phys.* **2022**, *24*, 19502–19511.

(61) Reck, G.; Dietz, G. THE ORDER-DISORDER STRUCTURE OF CARBAMAZEPINE DIHYDRATE-SH-DIBENZ B,F AZEPINE-5-CARBOXAMIDE DIHYDRATE, C<sub>15</sub>H<sub>12</sub>N<sub>2</sub>O<sub>2</sub>·2H<sub>2</sub>O. *Cryst. Res. Technol.* **1986**, *21*, 1463–1468.

(62) Sovago, I.; Gutmann, M. J.; Senn, H. M.; Thomas, L. H.; Wilson, C. C.; Farrugia, L. J. Electron density, disorder and polymorphism: high-resolution diffraction studies of the highly polymorphic neuralgic drug carbamazepine. *Acta Crystallogr., Sect. B: Struct. Sci., Cryst. Eng. Mater.* **2016**, *72*, 39–50.

(63) Laine, E.; Tuominen, V.; Ilvessalo, P.; Kahela, P. FORMATION OF DIHYDRATE FROM CARBAMAZEPINE ANHYDRATE IN AQUEOUS CONDITIONS. *Int. J. Pharm.* **1984**, *20*, 307–314.

(64) Nievergelt, P. P.; Spingler, B. Growing single crystals of small molecules by thermal recrystallization, a viable option even for minute amounts of material? *CrystEngComm* **2017**, *19*, 142–147.

(65) Takaiwa, D.; Hatano, I.; Koga, K.; Tanaka, H. Phase diagram of water in carbon nanotubes. *Proc. Natl. Acad. Sci. U. S. A.* **2008**, *105*, 39–43.

(66) Johnston, A.; Florence, A. J.; Kennedy, A. R. Carbamazepine N,N-dimethylformamide solvate. *Acta Crystallogr., Sect. E: Crystallogr. Commun.* **2005**, *61*, O1509–O1511.

(67) Johnston, A.; Johnston, B. F.; Kennedy, A. R.; Florence, A. J. Targeted crystallisation of novel carbamazepine solvates based on a retrospective Random Forest classification. *CrystEngComm* **2008**, *10*, 23–25.

(68) Johnston, A.; Florence, A. J.; Kennedy, A. R. Carbamazepine furfural hemisolvate. *Acta Crystallogr., Sect. E: Crystallogr. Commun.* **2005**, *61*, O1777–O1779.

(69) Lohani, S.; Zhang, Y. G.; Chyall, L. J.; Mougins-Andres, P.; Muller, F. X.; Grant, D. J. W. Carbamazepine-2,2,2-trifluoroethanol (1/1). *Acta Crystallogr., Sect. E: Crystallogr. Commun.* **2005**, *61*, O1310–O1312.

(70) Fernandes, P.; Bardin, J.; Johnston, A.; Florence, A. J.; Leech, C. K.; David, W. I. F.; Shankland, K. Carbamazepine trifluoroacetic acid solvate. *Acta Crystallogr., Sect. E: Struct. Rep. Online* **2007**, *63*, O4269–U2927.

(71) Bingham, A. L.; Hughes, D. S.; Hursthouse, M. B.; Lancaster, R. W.; Tavener, S.; Threlfall, T. L. Over one hundred solvates of sulfathiazole. *Chem. Commun.* **2001**, 603–604.

(72) Hughes, D. S.; Bingham, A. L.; Hursthouse, M. B.; Threlfall, T. L.; Bond, A. D. The extensive solid-form landscape of sulfathiazole: hydrogen-bond topology and node shape. *CrystEngComm* **2022**, *24*, 6587–6599.

(73) Bhardwaj, R. M.; Reutzel-Edens, S. M.; Johnston, B. F.; Florence, A. J. A random forest model for predicting crystal packing of olanzapine solvates. *CrystEngComm* **2018**, *20*, 3947–3950.

(74) Reutzel-Edens, S. M.; Bhardwaj, R. M. Crystal forms in pharmaceutical applications: olanzapine, a gift to crystal chemistry that keeps on giving. *IUCr.* **2020**, *7*, 955–964.

(75) Bhardwaj, R. M.; McMahon, J. A.; Nyman, J.; Price, L. S.; Konar, S.; Oswald, I. D. H.; Pulham, C. R.; Price, S. L.; Reutzel-Edens, S. M. A Prolific Solvate Former, Galunisertib, under the Pressure of Crystal Structure Prediction, Produces Ten Diverse Polymorphs. *J. Am. Chem. Soc.* **2019**, *141*, 13887–13897.

(76) Chisholm, J. A.; Motherwell, S. < i > COMPACK</i>: a program for identifying crystal structure similarity using distances. *J. Appl. Crystallogr.* **2005**, *38*, 228–231.

(77) Gelbrich, T.; Hursthouse, M. B. Systematic investigation of the relationships between 25 crystal structures containing the carbamazepine molecule or a close analogue: a case study of the XPac method. *CrystEngComm* **2006**, *8*, 448–460.

(78) Rapeenun, P.; Rarey, J.; Flood, A. E. Shortcut Method for the Prediction of the Cocrystal Solubility Line. *Cryst. Growth Des.* **2021**, *21*, 5534–5543.

(79) Good, D. J.; Rodriguez-Hornedo, N. Solubility Advantage of Pharmaceutical Cocrystals. *Cryst. Growth Des.* **2009**, *9*, 2252–2264.

(80) Omori, M.; Yamamoto, H.; Matsui, F.; Sugano, K. Dissolution Profiles of Carbamazepine Cocrystals with Cis-Trans Isomeric Cofomers. *Pharm. Res.* **2023**, *40*, 579–591.

(81) Alvani, A.; Shayanfar, A. Solution Stability of Pharmaceutical Cocrystals. *Cryst. Growth Des.* **2022**, *22*, 6323–6337.

(82) Khajir, S.; Shayanfar, A.; Monajjemzadeh, F.; Jouyban, A. Crystal engineering of valproic acid and carbamazepine to improve hygroscopicity and dissolution profile. *Drug Dev. Ind. Pharm.* **2021**, *47*, 1674–1679.

(83) Sathisaran, I.; Dalvi, S. V. Cocrystallization of carbamazepine with amides: Cocrystal and eutectic phases with improved dissolution. *J. Mol. Struct.* **2019**, *1193*, 398–415.



- (84) Sabouri, S.; Shayanfar, A. Effects of Surfactant and Polymer on Thermodynamic Solubility and Solution Stability of Carbamazepine-Cinnamic Acid Cocrystal. *Pharm. Chem. J.* **2022**, *56*, 913–917.
- (85) Almarsson, O.; Zaworotko, M. J. Crystal engineering of the composition of pharmaceutical phases. Do pharmaceutical co-crystals represent a new path to improved medicines? *Chem. Commun.* **2004**, 1889–1896.
- (86) Dai, X. L.; Chen, J. M.; Lu, T. B. Pharmaceutical cocrystallization: an effective approach to modulate the physicochemical properties of solid-state drugs. *CrystEngComm* **2018**, *20*, 5292–5316.
- (87) Sugden, I. J.; Braun, D. E.; Bowskill, D. H.; Adjiman, C. S.; Pantelides, C. C. Efficient Screening of Coformers for Active Pharmaceutical Ingredient Cocrystallization. *Cryst. Growth Des.* **2022**, *22*, 4513–4527.
- (88) Martins, I. C. B.; Emmerling, F. Carbamazepine Dihydroxybenzoic Acid Cocrystals: Exploring Packing Interactions and Reaction Kinetics. *Cryst. Growth Des.* **2021**, *21*, 6961–6970.
- (89) Rajbongshi, T.; Sarmah, K. K.; Das, S.; Deka, P.; Saha, A.; Saha, B. K.; Puschmann, H.; Reddy, C. M.; Thakuria, R. Non-stoichiometric carbamazepine cocrystal hydrates of 3,4-/3,5-dihydroxybenzoic acids: coformer-water exchange. *Chem. Commun.* **2023**, *59*, 3902–3905.
- (90) Lee, C.; Cho, A. Y.; Yoon, W.; Yun, H.; Kang, J. W.; Lee, J. Crystallization via Resorcinol-Urea Interactions: Naringenin and Carbamazepine. *Cryst. Growth Des.* **2019**, *19*, 3807–3814.
- (91) Lee, C. C.; Lim, J. H.; Cho, A. Y.; Yoon, W.; Yun, H. S.; Kang, J. W.; Lee, J. H. Molecular structures of flavonoid co-formers for cocrystallization with carbamazepine. *J. Ind. Eng. Chem.* **2023**, *118*, 309–317.
- (92) Etter, M. C. ENCODING AND DECODING HYDROGEN-BOND PATTERNS OF ORGANIC-COMPOUNDS. *Acc. Chem. Res.* **1990**, *23*, 120–126.
- (93) Rahim, S. A.; Hammond, R. B.; Sheikh, A. Y.; Roberts, K. J. A comparative assessment of the influence of different crystallization screening methodologies on the solid forms of carbamazepine co-crystals. *CrystEngComm* **2013**, *15*, 3862–3873.
- (94) Guerain, M.; Derollez, P.; Roca-Paixao, L.; Dejoie, C.; Correia, N. T.; Affouard, F. Structure determination of a new cocrystal of carbamazepine and DL-tartaric acid by synchrotron powder X-ray diffraction. *Acta Crystallogr., Sect. C: Struct. Chem.* **2020**, *76*, 225–230.
- (95) Horst, J. H. ter; Cains, P. W. Co-crystal polymorphs from a solvent-mediated transformation. *Cryst. Growth Des.* **2008**, *8*, 2537–2542.
- (96) Habgood, M.; Deij, M. A.; Mazurek, J.; Price, S. L.; ter Horst, J. H. Carbamazepine Co-crystallization with Pyridine Carboxamides: Rationalization by Complementary Phase Diagrams and Crystal Energy Landscapes. *Cryst. Growth Des.* **2010**, *10*, 903–912.
- (97) Porter, W. W.; Elie, S. C.; Matzger, A. J. Polymorphism in carbamazepine cocrystals. *Cryst. Growth Des.* **2008**, *8*, 14–16.
- (98) Pagire, S. K.; Jadav, N.; Vangala, V. R.; Whiteside, B.; Paradkar, A. Thermodynamic Investigation of Carbamazepine-Saccharin Co-Crystal Polymorphs. *J. Pharm. Sci.* **2017**, *106*, 2009–2014.
- (99) Padrela, L. M.; Castro-Dominguez, B.; Ziaee, A.; Long, B.; Ryan, K. M.; Walker, G.; O'Reilly, E. J. Co-crystal polymorphic control by nanodroplet and electrical confinement. *CrystEngComm* **2019**, *21*, 2845–2848.
- (100) Wang, X. J.; Du, S. Z.; Zhang, R.; Jia, X. D.; Yang, T.; Zhang, X. J. Drug-drug cocrystals: Opportunities and challenges. *Asian J. Pharm. Sci.* **2021**, *16*, 307–317.
- (101) Aljohani, M.; Pallipurath, A. R.; McArdle, P.; Erxleben, A. A Comprehensive Cocrystal Screening Study of Chlorothiazide. *Cryst. Growth Des.* **2017**, *17*, 5223–5232.
- (102) Nicolai, B.; Fournier, B.; Dahaoui, S.; Gillet, J. M.; Ghermani, N. E. Crystal and Electron Properties of Carbamazepine-Aspirin Co-crystal. *Cryst. Growth Des.* **2019**, *19*, 1308–1321.
- (103) Majumder, M.; Buckton, G.; Rawlinson-Malone, C.; Williams, A. C.; Spillman, M. J.; Shankland, N.; Shankland, K. A carbamazepine-indomethacin (1:1) cocrystal produced by milling. *CrystEngComm* **2011**, *13*, 6327–6328.
- (104) Chen, A.; Cai, P. S.; Luo, M. Q.; Guo, M. S.; Cai, T. Melt Crystallization of Celecoxib-Carbamazepine Cocrystals with the Synchronized Release of Drugs. *Pharm. Res.* **2023**, *40*, 567–577.
- (105) Delori, A.; Galek, P. T. A.; Pidcock, E.; Patni, M.; Jones, W. Knowledge-based hydrogen bond prediction and the synthesis of salts and cocrystals of the anti-malarial drug pyrimethamine with various drug and GRAS molecules. *CrystEngComm* **2013**, *15*, 2916–2928.
- (106) Huang, D. D.; Chan, H. C. S.; Wu, Y. S.; Li, L.; Zhang, L.; Lv, Y.; Yang, X. M.; Zhou, Z. Z. Phase solubility investigation and theoretical calculations on drug-drug cocrystals of carbamazepine with Emodin, Paeonol. *J. Mol. Liq.* **2021**, *329*, No. 115604.
- (107) Makadia, J.; Seaton, C. C.; Li, M. Z. Apigenin Cocrystals: From Computational Prescreening to Physicochemical Property Characterization. *Cryst. Growth Des.* **2023**, *23*, 3480–3495.
- (108) Buist, A. R.; Kennedy, A. R.; Shankland, K.; Shankland, N.; Spillman, M. J. Salt Forms of Amides: Protonation and Polymorphism of Carbamazepine and Cytenamide. *Cryst. Growth Des.* **2013**, *13*, 5121–5127.
- (109) Dalpiaz, A.; Ferretti, V.; Bertolasi, V.; Pavan, B.; Monari, A.; Pastore, M. From Physical Mixtures to Co-Crystals: How the Coformers Can Modify Solubility and Biological Activity of Carbamazepine. *Mol. Pharmaceutics* **2018**, *15*, 268–278.
- (110) Steed, J. W. 21st century developments in the understanding and control of molecular solids. *Chem. Commun.* **2018**, *54*, 13175–13182.
- (111) Metherall, J. P.; Carroll, R. C.; Coles, S. J.; Hall, M. J.; Probert, M. R. Advanced crystallisation methods for small organic molecules. *Chem. Soc. Rev.* **2023**, *52*, 1995–2010.
- (112) Florence, A. J.; Johnston, A.; Price, S. L.; Nowell, H.; Kennedy, A. R.; Shankland, N. An automated parallel crystallisation search for predicted crystal structures and packing motifs of carbamazepine. *J. Pharm. Sci.* **2006**, *95*, 1918–1930.
- (113) Neumann, M. A.; van de Streek, J.; Fabbiani, F. P. A.; Hidber, P.; Grassmann, O. Combined crystal structure prediction and high-pressure crystallization in rational pharmaceutical polymorph screening. *Nat. Commun.* **2015**, *6*, 7793.
- (114) Taylor, C. R.; Mulvee, M. T.; Perenyi, D. S.; Probert, M. R.; Day, G. M.; Steed, J. W. Minimizing Polymorphic Risk through Cooperative Computational and Experimental Exploration. *J. Am. Chem. Soc.* **2020**, *142*, 16668–16680.
- (115) Jiang, Q.; Ward, M. D. Crystallization under nanoscale confinement. *Chem. Soc. Rev.* **2014**, *43*, 2066–2079.
- (116) Fellah, N.; Dela Cruz, I. J. C.; Alamani, B. G.; Shtukenberg, A. G.; Pandit, A. V.; Ward, M. D.; Myerson, A. S. Crystallization and Polymorphism under Nanoconfinement. *Cryst. Growth Des.* **2024**, *24*, 3527–3558.
- (117) Tyler, A. R.; Ragbirsingh, R.; McMonagle, C. J.; Waddell, P. G.; Heaps, S. E.; Steed, J. W.; Thaw, P.; Hall, M. J.; Probert, M. R. High-Throughput Oil-Encapsulated Nanodroplet Crystallisation for Organic Organic-Soluble Small Molecule Structure Elucidation and Polymorph Screening. *Chem.* **2020**, *6*, 1755–1765.
- (118) Diao, Y.; Whaley, K. E.; Helgeson, M. E.; Woldeyes, M. A.; Doyle, P. S.; Myerson, A. S.; Hatton, T. A.; Trout, B. L. Gel-Induced Selective Crystallization of Polymorphs. *J. Am. Chem. Soc.* **2012**, *134*, 673–684.
- (119) Ward, M. R.; Taylor, C. R.; Mulvee, M. T.; Lampronti, G. I.; Belenguer, A. M.; Steed, J. W.; Day, G. M.; Oswald, I. D. H. Pushing Technique Boundaries to Probe Conformational Polymorphism. *Cryst. Growth Des.* **2023**, *23*, 7217–7230.
- (120) Trasi, N. S.; Abbou Oucherif, K.; Litster, J. D.; Taylor, L. S. Evaluating the influence of polymers on nucleation and growth in supersaturated solutions of acetaminophen. *CrystEngComm* **2015**, *17*, 1242–1248.
- (121) Frank, D. S.; Zhu, Q. Y.; Matzger, A. J. Inhibiting or Accelerating Crystallization of Pharmaceuticals by Manipulating Polymer Solubility. *Mol. Pharmaceutics* **2019**, *16*, 3720–3725.
- (122) Levesque, A.; Maris, T.; Wuest, J. D. ROY Reclaims Its Crown: New Ways To Increase Polymorphic Diversity. *J. Am. Chem. Soc.* **2020**, *142*, 11873–11883.



- (123) Villeneuve, N. M.; Dickman, J.; Maris, T.; Day, G. M.; Wuest, J. D. Seeking Rules Governing Mixed Molecular Crystallization. *Cryst. Growth Des.* **2023**, *23*, 273–288.
- (124) Hill, A.; Kras, W.; Theodosiou, F.; Wanat, M.; Lee, D. N.; Cruz-Cabeza, A. J. Polymorphic Solid Solutions in Molecular Crystals: Tips, Tricks, and Switches. *J. Am. Chem. Soc.* **2023**, *145*, 20562–20577.
- (125) Foster, J. A.; Piepenbrock, M. O. M.; Lloyd, G. O.; Clarke, N.; Howard, J. A. K.; Steed, J. W. Anion-switchable supramolecular gels for controlling pharmaceutical crystal growth. *Nat. Chem.* **2010**, *2*, 1037–1043.
- (126) Nicholson, C. E.; Chen, C.; Mendis, B.; Cooper, S. J. Stable Polymorphs Crystallized Directly under Thermodynamic Control in Three-Dimensional Nanoconfinement: A Generic Methodology. *Cryst. Growth Des.* **2011**, *11*, 363–366.
- (127) Maunder, J. J.; Aguilar, J. A.; Hodgkinson, P.; Cooper, S. J. Structured ternary fluids as nanocrystal incubators for enhanced crystallization control. *Chem. Sci.* **2022**, *13*, 13132.
- (128) Potticary, J.; Hall, C.; Hamilton, V.; McCabe, J. F.; Hall, S. R. Crystallisation From Volatile Deep Eutectic Solvents. *Cryst. Growth Des.* **2020**, *20*, 2877–2884.
- (129) Potticary, J.; Hall, C. L.; Guo, R.; Price, S. L.; Hall, S. R. On the Application of Strong Magnetic Fields during Organic Crystal Growth. *Cryst. Growth Des.* **2021**, *21*, 6254–6265.
- (130) Samara, M.; Nasser, A.; Mingelgrin, U. Mechanochemical removal of carbamazepine. *Chemosphere* **2016**, *160*, 266–272.
- (131) Ostwald, W. Z. The formation and changes of solids. *Phys. Chem.* **1897**, *22*, 289–330.
- (132) Fellah, N.; Dela Cruz, I. J. C.; Alamani, B. G.; Shtukenberg, A. G.; Pandit, A. V.; Ward, M. D.; Myerson, A. S. Crystallization and Polymorphism under Nanoconfinement. *Cryst. Growth Des.* **2024**, *24*, 3527.
- (133) Belenguer, A. M.; Lampronti, G. I.; Cruz-Cabeza, A. J.; Hunter, C. A.; Sanders, J. K. M. Solvation and surface effects on polymorph stabilities at the nanoscale. *Chem. Sci.* **2016**, *7*, 6617–6627.
- (134) Tyler, A. R.; Ragbirsingh, R.; McMonagle, C. J.; Waddell, P. G.; Heaps, S. E.; Steed, J. W.; Thaw, P.; Hall, M. J.; Probert, M. R. Encapsulated Nanodroplet Crystallization of Organic-Soluble Small Molecules. *Chem.* **2020**, *6*, 1755–1765.
- (135) Beran, G. J. O.; Sugden, I. J.; Greenwell, C.; Bowskill, D. H.; Pantelides, C. C.; Adjiman, C. S. How many more polymorphs of ROY remain undiscovered. *Chem. Sci.* **2022**, *13*, 1288–1297.
- (136) Foster, J. A.; Damodaran, K. K.; Maurin, A.; Day, G. M.; Thompson, H. P. G.; Cameron, G. J.; Bernal, J. C.; Steed, J. W. Pharmaceutical polymorph control in a drug-mimetic supramolecular gel. *Chem. Sci.* **2017**, *8*, 78–84.
- (137) Chen, C.; Cook, O.; Nicholson, C. E.; Cooper, S. J. Leapfrogging Ostwald's Rule of Stages: Crystallization of Stable  $\gamma$ -Glycine Directly from Microemulsions. *Cryst. Growth Des.* **2011**, *11*, 2228–2237.
- (138) Nicholson, C. E.; Cooper, S. J. Crystallization of Mefenamic Acid from Dimethylformamide Microemulsions: Obtaining Thermodynamic Control through 3D Nanoconfinement. *Crystals* **2011**, *1*, 195–205.
- (139) Parkes, A.; Ziaee, A.; Walker, G.; O'Reilly, E. Controlled isolation and stabilisation of pure metastable carbamazepine form IV by droplet-confinement via a continuous manufacturing route. *CrystEngComm* **2022**, *24*, 6825–6829.
- (140) Hasa, D.; Jones, W. Screening for new pharmaceutical solid forms using mechanochemistry: A practical guide. *Adv. Drug Delivery Rev.* **2017**, *117*, 147–161.
- (141) James, S. L.; Adams, C. J.; Bolm, C.; Braga, D.; Collier, P.; Friscic, T.; Grepioni, F.; Harris, K. D. M.; Hyett, G.; Jones, W.; Krebs, A.; Mack, J.; Maini, L.; Orpen, A. G.; Parkin, I. P.; Shearouse, W. C.; Steed, J. W.; Waddell, D. C. Mechanochemistry: opportunities for new and cleaner synthesis. *Chem. Soc. Rev.* **2012**, *41*, 413–447.
- (142) Belenguer, A. M.; Cruz-Cabeza, A. J.; Lampronti, G. I.; Sanders, J. K. M. On the prevalence of smooth polymorphs at the nanoscale: implications for pharmaceuticals. *CrystEngComm* **2019**, *21*, 2203–2211.
- (143) Bysouth, S. R.; Bis, J. A.; Igo, D. Cocrystallization via planetary milling: Enhancing throughput of solid-state screening methods. *Int. J. Pharm.* **2011**, *411*, 169–171.
- (144) Long, B.; Walker, G. M.; Ryan, K. M.; Padrela, L. Controlling Polymorphism of Carbamazepine Nanoparticles in a Continuous Supercritical-CO<sub>2</sub>-Assisted Spray Drying Process. *Cryst. Growth Des.* **2019**, *19*, 3755–3767.
- (145) Long, B.; Ryan, K. M.; Padrela, L. Investigating Process Variables and Additive Selection To Optimize Polymorphic Control of Carbamazepine in a CO<sub>2</sub> Antisolvent Crystallization Process. *Org. Process Res. Dev.* **2020**, *24*, 1006–1017.
- (146) Schrode, B.; Bodak, B.; Riegler, H.; Zimmer, A.; Christian, P.; Werzer, O. Solvent Vapor Annealing of Amorphous Carbamazepine Films for Fast Polymorph Screening and Dissolution Alteration. *ACS Omega* **2017**, *2*, 5582–5590.
- (147) Neumann, M. A.; Leusen, F. J. J.; Kendrick, J. A major advance in crystal structure prediction. *Angew. Chem., Int. Ed.* **2008**, *47*, 2427–2430.
- (148) Nyman, J.; Reutzel-Edens, S. M. Crystal structure prediction is changing from basic science to applied technology. *Faraday Discuss.* **2018**, *211*, 459–476.
- (149) Yang, M. J.; Dybeck, E.; Sun, G. X.; Peng, C. W.; Samas, B.; Burger, V. M.; Zeng, Q.; Jin, Y. D.; Bellucci, M. A.; Liu, Y.; Zhang, P. Y.; Ma, J.; Jiang, Y. A.; Hancock, B. C.; Wen, S. H.; Wood, G. P. F. Prediction of the Relative Free Energies of Drug Polymorphs above Zero Kelvin. *Cryst. Growth Des.* **2020**, *20*, 5211–5224.
- (150) Bowskill, D. H.; Sugden, I. J.; Konstantinopoulos, S.; Adjiman, C. S.; Pantelides, C. C. Crystal Structure Prediction Methods for Organic Molecules: State of the Art. *Annu. Rev. Chem. Biomol. Eng.* **2021**, *12*, 593–623.
- (151) Beran, G. J. O. Frontiers of molecular crystal structure prediction for pharmaceuticals and functional organic materials. *Chem. Sci.* **2023**, *14*, 13290–13312.
- (152) Firaha, D.; Liu, Y. M.; van de Streek, J.; Sasikumar, K.; Dietrich, H.; Helfferich, J.; Aerts, L.; Braun, D. E.; Broo, A.; DiPasquale, A. G.; Lee, A. Y.; Le Meur, S.; Lill, S. O. N.; Lunsmann, W. J.; Mattei, A.; Muglia, P.; Putra, O. D.; Raoui, M.; Reutzel-Edens, S. M.; Rome, S.; Sheikh, A. Y.; Tkatchenko, A.; Woollam, G. R.; Neumann, M. A. Predicting crystal form stability under real-world conditions. *Nature* **2023**, *623*, 324.
- (153) Cruz-Cabeza, A. J.; Day, G. M.; Motherwell, W. D. S.; Jones, W. Amide pyramidalization in carbamazepine: A flexibility problem in crystal structure prediction? *Cryst. Growth Des.* **2006**, *6*, 1858–1866.
- (154) Cruz-Cabeza, A. J.; Day, G. M.; Motherwell, W. D. S.; Jones, W. Importance of molecular shape for the overall stability of hydrogen bond motifs in the crystal structures of various carbamazepine-type drug molecules. *Cryst. Growth Des.* **2007**, *7*, 100–107.
- (155) Florence, A. J.; Leech, C. K.; Shankland, N.; Shankland, K.; Johnston, A. Control and prediction of packing motifs: a rare occurrence of carbamazepine in a catemeric configuration. *CrystEngComm* **2006**, *8*, 746–747.
- (156) Kras, W.; Carletta, A.; Montis, R.; Sullivan, R. A.; Cruz-Cabeza, A. J. Switching polymorph stabilities with impurities provides a thermodynamic route to benzamide form III. *Commun. Chem.* **2021**, *4*, 1–7.
- (157) Cruz-Cabeza, A. J.; Day, G. M.; Jones, W. Predicting Inclusion Behaviour and Framework Structures in Organic Crystals. *Chem.—Eur. J.* **2009**, *15*, 13033–13040.
- (158) Jones, J. T. A.; Hasell, T.; Wu, X. F.; Bacsá, J.; Jelfs, K. E.; Schmidtman, M.; Chong, S. Y.; Adams, D. J.; Trewin, A.; Schiffman, F.; Cora, F.; Slater, B.; Steiner, A.; Day, G. M.; Cooper, A. I. Modular and predictable assembly of porous organic molecular crystals. *Nature* **2011**, *474*, 367–371.
- (159) Berzins, A.; Zvanina, D.; Trimdale, A. Detailed Analysis of Packing Efficiency Allows Rationalization of Solvate Formation Propensity for Selected Structurally Similar Organic Molecules. *Cryst. Growth Des.* **2018**, *18*, 2040–2045.
- (160) Braun, D. E.; Lingireddy, S. R.; Beidelschies, M. D.; Guo, R.; Muller, P.; Price, S. L.; Reutzel-Edens, S. M. Unraveling Complexity in

the Solid Form Screening of a Pharmaceutical Salt: Why so Many Forms? Why so Few? *Cryst. Growth Des.* **2017**, *17*, 5349–5365.

(161) van Eijck, B. P.; Kroon, J. Structure predictions allowing more than one molecule in the asymmetric unit. *Acta Crystallogr., Sect. B: Struct. Sci.* **2000**, *56*, 535–542.

(162) Leusen, F. J. J. Crystal structure prediction of diastereomeric salts: A step toward rationalization of racemate resolution. *Cryst. Growth Des.* **2003**, *3*, 189–192.

(163) Karamertzanis, P. G.; Price, S. L. Challenges of crystal structure prediction of diastereomeric salt pairs. *J. Phys. Chem. B* **2005**, *109*, 17134–17150.

(164) Cruz-Cabeza, A. J.; Day, G. M.; Jones, W. Towards Prediction of Stoichiometry in Crystalline Multicomponent Complexes. *Chem.—Eur. J.* **2008**, *14*, 8830–8836.

(165) Cruz-Cabeza, A. J.; Karki, S.; Fabián, L.; Friscic, T.; Day, G. M.; Jones, W. Predicting stoichiometry and structure of solvates. *Chem. Commun.* **2010**, *46*, 2224–2226.

(166) Dybeck, E. C.; Thiel, A.; Schnieders, M. J.; Pickard, F. C.; Wood, G. P. F.; Krzyzaniak, J. F.; Hancock, B. C. A Comparison of Methods for Computing Relative Anhydrous-Hydrate Stability with Molecular Simulation. *Cryst. Growth Des.* **2023**, *23*, 142–167.

(167) Greenwell, C.; McKinley, J. L.; Zhang, P. Y.; Zeng, Q.; Sun, G. X.; Li, B. C.; Wen, S. H.; Beran, G. J. O. Overcoming the difficulties of predicting conformational polymorph energetics in molecular crystals via correlated wavefunction methods. *Chem. Sci.* **2020**, *11*, 2200–2214.

(168) Butler, P. W. V.; Day, G. M. Reducing overprediction of molecular crystal structures via threshold clustering. *Proc. Natl. Acad. Sci. U. S. A.* **2023**, *120*, e2300516120.

(169) Francia, N. F.; Price, L. S.; Nyman, J.; Price, S. L.; Salvalaglio, M. Systematic Finite-Temperature Reduction of Crystal Energy Landscapes. *Cryst. Growth Des.* **2020**, *20*, 6847–6862.

(170) Montis, R.; Davey, R. J.; Wright, S. E.; Woollam, G. R.; Cruz-Cabeza, A. J. Transforming Computed Energy Landscapes into Experimental Realities: The Role of Structural Rugosity. *Angew. Chem., Int. Ed.* **2020**, *59*, 20357–20360.

(171) Burcham, L.; Doherty, M. F.; Peters, B. G.; Price, S. L.; Salvalaglio, M.; Reutzler-Edens, S. M.; Price, L. S.; Addula, R. K. R.; Francia, N.; Khanna, V. Pharmaceutical Digital Design: From Chemical Structure through Crystal Polymorph to Conceptual Crystallization Process. *ChemRxiv*, ver. 1, January 23, 2024. .

(172) Khoo, J. Y.; Shah, U. V.; Schaeperstoens, M.; Williams, D. R.; Heng, J. Y. Y. Process-induced phase transformation of carbamazepine dihydrate to its polymorphic anhydrides. *Powder Technol.* **2013**, *236*, 114–121.

(173) Surana, R.; Pyne, A.; Suryanarayanan, R. Solid-vapor interactions: Influence of environmental conditions on the dehydration of carbamazepine dihydrate. *AAPS PharmSciTech* **2003**, *4*, 539.

(174) Han, J.; Suryanarayanan, R. Influence of Environmental Conditions on the Kinetics and Mechanism of Dehydration of Carbamazepine Dihydrate. *Pharm. Dev. Technol.* **1998**, *3*, 587–596.

(175) Tian, F.; Zeitler, J. A.; Strachan, C. J.; Saville, D. J.; Gordon, K. C.; Rades, T. Characterizing the conversion kinetics of carbamazepine polymorphs to the dihydrate in aqueous suspension using Raman spectroscopy. *J. Pharm. Biomed. Anal.* **2006**, *40*, 271–280.

(176) Murphy, D.; Rodríguez-Cintrón, F.; Langevin, B.; Kelly, R. C.; Rodríguez-Hornedo, N. Solution-mediated phase transformation of anhydrous to dihydrate carbamazepine and the effect of lattice disorder. *Int. J. Pharm.* **2002**, *246*, 121–134.

(177) Benmore, C. J.; Edwards, A.; Alderman, O. L. G.; Cherry, B. R.; Smith, P.; Smith, D.; Byrn, S.; Weber, R.; Yarger, J. L. The Structure of Liquid and Glassy Carbamazepine. *Quantum Beam Sci.* **2022**, *6*, 31.

(178) Silski-Devlin, A. M.; Petersen, J. P.; Liu, J.; Turner, G. A.; Poutsma, J. C.; Kandel, S. A. Hydrogen-Bonded Tetramers of Carbamazepine. *J. Phys. Chem. C* **2020**, *124*, 5213–5219.

(179) Jensen, L. G.; Skautrup, F. B.; Müllertz, A.; Abrahamsson, B.; Rades, T.; Priemel, P. A. Amorphous is not always better—A dissolution study on solid state forms of carbamazepine. *Int. J. Pharm.* **2017**, *522*, 74–79.

(180) Goodwin, M. J.; Musa, O. M.; Berry, D. J.; Steed, J. W. Small-Molecule Povidone Analogues in Coamorphous Pharmaceutical Phases. *Cryst. Growth Des.* **2018**, *18*, 701–709.

(181) Rodrigues Sá Couto, A.; Ryzhakov, A.; Larsen, K. L.; Loftsson, T. Interaction of Native Cyclodextrins and Their Hydroxypropylated Derivatives with Carbamazepine in Aqueous Solution. Evaluation of Inclusion Complexes and Aggregates Formation. *ACS Omega* **2019**, *4*, 1460–1469.

(182) Varughese, S.; Kiran, M.; Ramamurty, U.; Desiraju, G. R. Nanoindentation in Crystal Engineering: Quantifying Mechanical Properties of Molecular Crystals. *Angew. Chem., Int. Ed.* **2013**, *52*, 2701–2712.

(183) Ramamurty, U.; Jang, J. I. Nanoindentation for probing the mechanical behavior of molecular crystals—a review of the technique and how to use it. *CrystEngComm* **2014**, *16*, 12–23.

(184) Gabriele, B. P. A.; Williams, C.; Lauer, M. E.; Derby, B.; Cruz-Cabeza, A. J. Nanoindentation of Molecular Crystals: Lessons Learned from Aspirin. *Cryst. Growth Des.* **2020**, *20*, 5956–5966.

(185) Reddy, C. M.; Krishna, G. R.; Ghosh, S. Mechanical properties of molecular crystals—applications to crystal engineering. *CrystEngComm* **2010**, *12*, 2296–2314.

(186) Krishna, G. R.; Devarapalli, R.; Lal, G.; Reddy, C. M. Mechanically Flexible Organic Crystals Achieved by Introducing Weak Interactions in Structure: Supramolecular Shape Synthons. *J. Am. Chem. Soc.* **2016**, *138*, 13561–13567.

(187) Sun, C. C.; Hou, H. Improving mechanical properties of caffeine and methyl gallate crystals by cocrystallization. *Cryst. Growth Des.* **2008**, *8*, 1575–1579.

(188) Bejoymohandas, K. S.; Redhu, A.; Sharma, C. H.; Seethalekshmi, S.; Divya, I. S.; Kiran, M.; Thalakulam, M.; Monti, F.; Nair, R. V.; Varughese, S. Polymorphism-driven Distinct Nano-mechanical, Optical, Photophysical, and Conducting Properties in a Benzothioephene-quinoline. *Chem. - Eur. J.* **2024**, *30*, e202303558.

(189) Gabriele, B. P. A.; Williams, C. J.; Lauer, M. E.; Derby, B.; Cruz-Cabeza, A. J. Impact of polymorphism on mechanical properties of molecular crystals: a study of *p*-amino and *m*-nitro benzoic acid with nanoindentation. *CrystEngComm* **2021**, *23*, 2027–2033.

(190) Divya, I. S.; Kandasamy, S.; Hasebe, S.; Sasaki, T.; Koshima, H.; Wozniak, K.; Varughese, S. Flexible organic crystals. Understanding the tractable co-existence of elastic and plastic bending. *Chem. Sci.* **2022**, *13*, 8989–9003.

(191) Gabriele, B. P. A.; Williams, C. J.; Lauer, M. E.; Derby, B.; Cruz-Cabeza, A. J. Probing anisotropic mechanical behaviour in carbamazepine form III. *CrystEngComm* **2021**, *23*, 5826–5838.

(192) Clara, M.; Strenn, B.; Kreuzinger, N. Carbamazepine as a possible anthropogenic marker in the aquatic environment: investigations on the behaviour of Carbamazepine in wastewater treatment and during groundwater infiltration. *Water Res.* **2004**, *38*, 947–954.

(193) He, Q.; Liang, J.-J.; Chen, L.-X.; Chen, S.-L.; Zheng, H.-L.; Liu, H.-X.; Zhang, H.-J. Removal of the environmental pollutant carbamazepine using molecular imprinted adsorbents: Molecular simulation, adsorption properties, and mechanisms. *Water Res.* **2020**, *168*, No. 115164.

(194) Décima, M. A.; Marzeddu, S.; Barchiesi, M.; Di Marcantonio, C.; Chiavola, A.; Boni, M. R. A Review on the Removal of Carbamazepine from Aqueous Solution by Using Activated Carbon and Biochar. *Sustainability* **2021**, *13*, 11760.